ISSN 2410-3438

Volume 7, Issue 21 – July – December - 2020

Journal of Quantitative and Statistical Analysis

ECORFAN®

Journal of Quantitative and Statistical Analysis, Volume 7, Issue 21, July - December 2020, is a journal edited six monthly by ECORFAN-Bolivia. 21 Loa 1179, Cd. Sucre. Chuquisaca, Bolivia. WEB: www.ecorfan.org, revista@ecorfan.org. Chief Editor: MIRANDA - TORRADO, Fernando. PhD. ISSN-On line: 2410-3438. Responsible for the latest update of this number ECORFAN Computer Unit. ESCAMILLA-BOUCHÁN, Imelda, PhD, LUNA-SOTO, Vladimir. PhD. Loa 1179, Cd. Sucre. Chuquisaca, Bolivia, last updated December 31, 2020.

Journal of Quantitative and Statistical Analysis

Definition of Journal

Scientific Objectives

Support the international scientific community in its written production Science, Technology and Innovation in the Field of Physical Sciences Mathematics and Earth sciences, in Subdisciplines of statistical analysis data analysis, multivariate analysis, statistic's and probability, statistical analytical, calculation.

ECORFAN-Mexico SC is a Scientific and Technological Company in contribution to the Human Resource training focused on the continuity in the critical analysis of International Research and is attached to CONACYT-RENIECYT number 1702902, its commitment is to disseminate research and contributions of the International Scientific Community, academic institutions, agencies and entities of the public and private sectors and contribute to the linking of researchers who carry out scientific activities, technological developments and training of specialized human resources with governments, companies and social organizations.

Encourage the interlocution of the International Scientific Community with other Study Centers in Mexico and abroad and promote a wide incorporation of academics, specialists and researchers to the publication in Science Structures of Autonomous Universities - State Public Universities - Federal IES - Polytechnic Universities - Technological Universities - Federal Technological Institutes - Normal Schools - Decentralized Technological Institutes - Intercultural Universities - S & T Councils - CONACYT Research Centers.

Scope, Coverage and Audience

Journal of Quantitative and Statistical Analysis is a Journal edited by ECORFAN-Mexico S.C in its Holding with repository in Bolivia, is a scientific publication arbitrated and indexed with semester periods. It supports a wide range of contents that are evaluated by academic peers by the Double-Blind method, around subjects related to the theory and practice of statistical analysis data analysis, multivariate analysis, statistic's and probability, statistical analytical, calculation with diverse approaches and perspectives, that contribute to the diffusion of the development of Science Technology and Innovation that allow the arguments related to the decision making and influence in the formulation of international policies in the Field of Physical Sciences Mathematics and Earth sciences. The editorial horizon of ECORFAN-Mexico® extends beyond the academy and integrates other segments of research and analysis outside the scope, as long as they meet the requirements of rigorous argumentative and scientific, as well as addressing issues of general and current interest of the International Scientific Society.

Editorial Board

Arbitration Committee

Assignment of Rights

The sending of an Article to Journal of Quantitative and Statistical Analysis emanates the commitment of the author not to submit it simultaneously to the consideration of other series publications for it must complement the Originality Format for its Article.

The authors sign the Authorization Format for their Article to be disseminated by means that ECORFAN-Mexico, S.C. In its Holding Bolivia considers pertinent for disclosure and diffusion of its Article its Rights of Work.

Declaration of Authorship

Indicate the Name of Author and Coauthors at most in the participation of the Article and indicate in extensive the Institutional Affiliation indicating the Department.

Identify the Name of Author and Coauthors at most with the CVU Scholarship Number-PNPC or SNI-CONACYT- Indicating the Researcher Level and their Google Scholar Profile to verify their Citation Level and H index.

Identify the Name of Author and Coauthors at most in the Science and Technology Profiles widely accepted by the International Scientific Community ORC ID - Researcher ID Thomson - arXiv Author ID - PubMed Author ID - Open ID respectively.

Indicate the contact for correspondence to the Author (Mail and Telephone) and indicate the Researcher who contributes as the first Author of the Article.

Plagiarism Detection

All Articles will be tested by plagiarism software PLAGSCAN if a plagiarism level is detected Positive will not be sent to arbitration and will be rescinded of the reception of the Article notifying the Authors responsible, claiming that academic plagiarism is criminalized in the Penal Code.

Arbitration Process

All Articles will be evaluated by academic peers by the Double Blind method, the Arbitration Approval is a requirement for the Editorial Board to make a final decision that will be final in all cases. MARVID® is a derivative brand of ECORFAN® specialized in providing the expert evaluators all of them with Doctorate degree and distinction of International Researchers in the respective Councils of Science and Technology the counterpart of CONACYT for the chapters of America-Europe-Asia- Africa and Oceania. The identification of the authorship should only appear on a first removable page, in order to ensure that the Arbitration process is anonymous and covers the following stages: Identification of the Journal with its author occupation rate - Identification of Authors and Coauthors - Detection of plagiarism PLAGSCAN - Review of Formats of Authorization and Originality-Allocation to the Editorial Board-Allocation of the pair of Expert Arbitrators-Notification of Arbitration -Declaration of observations to the Author-Verification of Article Modified for Editing-Publication.

Instructions for Scientific, Technological and Innovation Publication

Knowledge Area

The works must be unpublished and refer to topics of statistical analysis data analysis, multivariate analysis, statistic's and probability, statistical analytical, calculation and other topics related to Physical Sciences Mathematics and Earth sciences.

Presentation of the content

In the first article we present, *Methodology to calculate the intensity of the electric field generated in a double circuit High Voltage Alternating Current overhead transmission line*, by AGUILAR-MARIN, Jorge Luis, VERGARA-VÁZQUEZ, Julio Cesar, PADILLA-CANTERO, Jorge Gabriel and HERNÁNDEZ-GONZÁLEZ, Daniel, with adscription in the Universidad Autónoma del Estado de Morelos, Centro Nacional de Investigación y Desarrollo Tecnológico, Instituto Nacional de Electricidad y Energías Limpias and the Instituto Tecnológico de Toluca, in the next article we present, *Laboratory data statistical analysis from CECCS' patients with or without SARS-CoV-2 (COVID-19)*, by YAÑEZ-VARGAS Israel, DOÑATE-ÁLVAREZ Andrea, QUINTANILLA-DOMINGEZ Joel and AGUILERA-GONZÁLEZ Gabriel, with adscription in the Universidad Politécnica de Juventino Rosas, in the next article we present, *Analysis and automatic segmentation of images for lungs regions extraction in X-ray chest*, by QUINTANILLA-DOMÍNGUEZ, Joel, YAÑEZ-VARGAS, Juan Israel, BUTANDA-SERRANO, Miriam and SÁNCHEZ-TORRECITAS, Enrique, with adscription in the Universidad Politécnica de Juventino Rosas, in the next article we present, *Relationship between electrostatic powder coating thickness measurements at different points on uneven surfaces*, by LUÉVANO-CABRALES, Olga Lidia, SALAS-PÉREZ, Francisco Guillermo, JUÁREZ-DEL TORO, Raymundo and MORALES-VILLA, Julio César.

Content

Article **Journal of Quantitative and Statistical Analysis**
December, 2020 Vol.7 No.21 1-8

Methodology to calculate the intensity of the electric field generated in a double circuit High Voltage Alternating Current overhead transmission line

Metodología para calcular la intensidad del campo eléctrico generado en una línea de transmisión aérea de corriente alterna de alto voltaje de doble circuito

AGUILAR-MARIN, Jorge Luis†*[1], VERGARA-VÁZQUEZ, Julio Cesar[2], PADILLA-CANTERO, Jorge Gabriel[3] and HERNÁNDEZ-GONZÁLEZ, Daniel[4]

[1]*Universidad Autónoma del Estado de Morelos, Facultad de Ciencias Químicas e Ingeniería, Cuernavaca, México.*
[2]*Centro Nacional de Investigación y Desarrollo Tecnológico, Departamento de Ingeniería Mecánica, Cuernavaca, México.*
[3]*Instituto Nacional de Electricidad y Energías Limpias, Gerencia de Transmisión y Distribución, Cuernavaca, México.*
[4]*Tecnológico Nacional de México, Instituto Tecnológico de Toluca, Departamento de Metalmecánica, Metepec, México.*

ID 1st Author: *Jorge Luis, Aguilar-Marin* / **ORC ID**: 0000-0002-0235-6946, **Researcher ID Thomson**: ABD-4533-2020, **CVU CONACYT ID**: 1010823

ID 1st Coauthor: *Julio Cesar, Vergara-Vázquez* / **ORC ID**: 0000-0003-1524-7914, **Researcher ID Thomson**: ABD-5487-2020

ID 2nd Coauthor: *Jorge Gabriel, Padilla-Cantero* / **ORC ID**: 0000-0002-6414-9483, **Researcher ID Thomson**: ABD-5334-2020

ID 3rd Coauthor: *Daniel, Hernández-González* / **ORC ID**: 0000-0002-9641-2717, **Researcher ID Thomson**: ABH-1389-2020

DOI: 10.35429/JQSA.2020.21.7.1.8 Received October 14, 2020; Accepted December 29, 2020

Abstract

One of the parameters considered in the design of transmission lines is the distribution of its generated electric field. The following article presents a reference methodology that allows obtaining the electric field on the right-of-way of a High Voltage Alternating Current (HVAC) overhead transmission line, the methodology is developed based on the Load Simulation Method (MSC) and the Image Method. The results obtained present a difference of less than 2%. In this way a case study of a 230 kV HVAC double circuit transmission line presented, an optimization of the phases of the transmission line circuits is carried out to determine the most efficient configuration for obtaining the electric field density. The results obtained allow a configuration of n circuits, admitting the different nominal voltages of the HVAC lines.

Lines of transmission, Electric field strength, Phase of circuits, Electric field values

Resumen

Uno de los parámetros considerados en el diseño de las líneas de transmisión es la distribución de su campo eléctrico generado. El siguiente artículo presenta una metodología de referencia que permite la obtención del campo eléctrico sobre el derecho de vía de una línea de transmisión aérea de Corriente Alterna de Alto Voltaje (HVAC), la metodología se desarrolla con base al Método de Simulación de Carga (MSC) y el Método de las imágenes. Los resultados obtenidos presentan una diferencia menor al 2%. De esta manera se presenta un caso de estudio de una línea de transmisión de doble circuito de 230 kV de HVAC, se realiza una optimización de las fases de los circuitos de la línea de transmisión, para determinar la configuración más eficiente para la obtención de la intensidad de campo eléctrico. Los resultados obtenidos permiten una configuración de n circuitos, admitiendo las diferentes tensiones nominales de las líneas de HVAC.

Líneas de transmisión, Intensidad de campo eléctrico, Faseo de circuitos, Valores de campo eléctrico

Citation: AGUILAR-MARIN, Jorge Luis, VERGARA-VÁZQUEZ, Julio Cesar, PADILLA-CANTERO, Jorge Gabriel and HERNÁNDEZ-GONZÁLEZ, Daniel. Methodology to calculate the intensity of the electric field generated in a double circuit High Voltage Alternating Current overhead transmission line. Journal of Quantitative and Statistical Analysis. 2020. 7-21: 1-8

* Correspondence to Author (email: jorge.aguilar.itt@gmail.com)
† Researcher contributing as first author.

Introduction

HVAC transmission lines are used to transmit large amounts of electrical power over long distances between electrical substations (Samy, Radwan & Akef, 2017).

The length of the transmission line is a factor that impacts the parameters of the line and the associated losses (Ukil, 2015).

Another factor that affects the parameters for the design of HVAC transmission lines is the intensity of the electric field generated (Samy, Radwan & Akef, 2017). The intensity of the electric field in overhead transmission lines is generated by the electric charge that circulates through the phase conductors, the field lines move away from the positive charges and towards the negative charges, Figure 1 shows their distribution (Grainger & Stevenson, 1996).

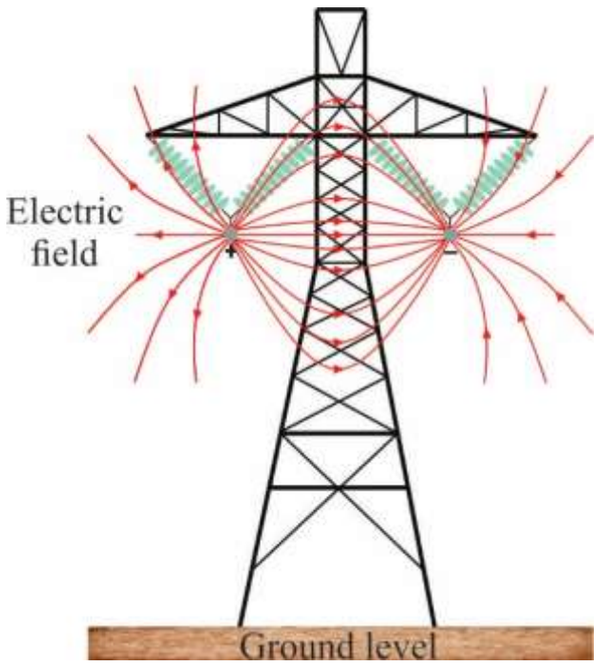

Figure 1 Electric field in an overhead transmission line
Source: Own Elaboration

The heights of the conductors are designed to keep the discharge currents below the recommended exposure values for people immersed in this field and any equipment that may be found on the right of way of the transmission line (Duncan & Malukutla, 2003), (Duncan & Malukutla, 1993).

Some countries have adopted recommended limits on electric field intensity, they are presented in Table 1 (IEC, 2014).

Country	Field value of phase to neutral, in kV/m
USA	30
Canada	25
Brazil	40

Table 1 Electric field values at ground level
Source: (IEC, 2014)

In accordance with (Sarma, 2000), an acceptable design should limit the electric field strength at ground level to 25 kV/m. It should be noted that these limits are only established from the point of view of human perception.

To determine the intensity of electric fields, most of the cases require commercial software, among which PLS CADD, ETAP, DIGSilent, among others, stand out.

The present work provides a methodology that allows the calculation of the intensity of the electric field don the right of way of an overhead HVAC transmission line.

Calculation methodology for electric field intensity

The following methodology allows determining the components of the intensity of the electric field, at a point (P) which is located on the right of way of a transmission line, given the location of the geometric coordinates (x, y), this point will be under the effect of the load $(q_k)$of the phase conductor located at the coordinates (x_k, y_k). In the same way the point (P) will be under the effect of negative charge $(-q_k)$ of the phase image conductor, located at the coordinates $(x_k, -y_k)$ (Adel & Dein, 2013).

The intensity of the electric field is calculated by means of the Charge Simulation Method (CSM), where the load (q_k) is distributed on the surface of the phase conductor. The principle pf this methodology is presented in Figure 2 (Ortiz, 2007).

For the calculation, it is considered that there is no free charge in space and that the permittivity of air (ε_0) is uniform and its conductivity is zero. In addition, the earth is considered a perfectly conductive surface where the effects of the image conductor are introduced (Adel & Dein, 2013), (Ortiz, 2007).

ISSN 2410-3438

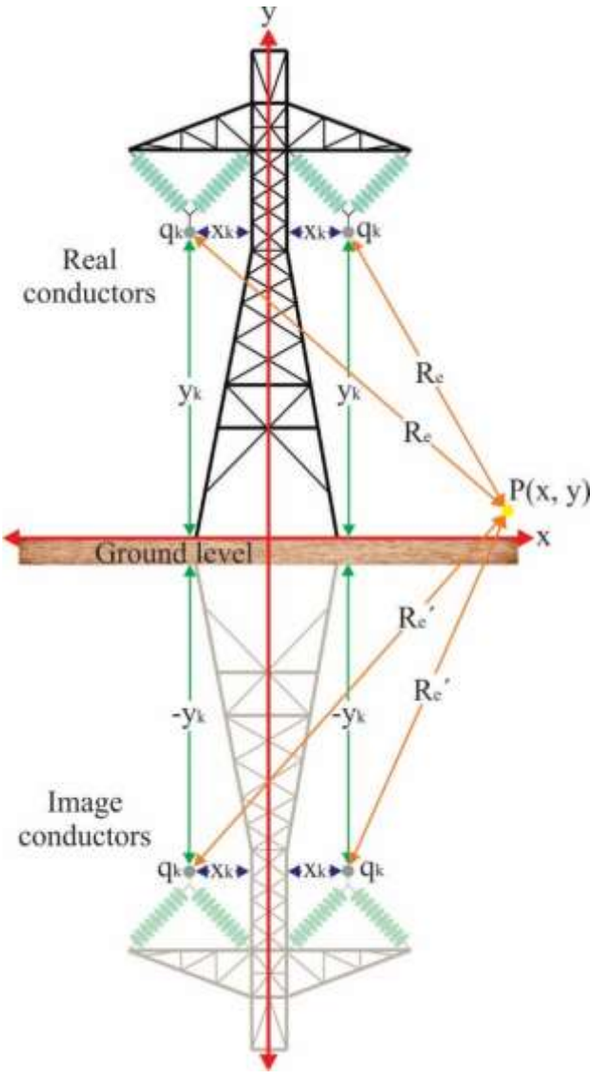

Figure 2 Geometric definition of variables.
Source: (Aguilar, Cisneros, Padilla & Vergara, 2020)

Where:

$y_k =$ Phase conductor height, in m.
$x_k =$ Horizontal distance from the phase conductor to the reference Y axis, in m.
$P =$ Point where you want to know the electric field intensity, in m.
$R_e =$ Distance between the phase conductor and point P, in m.
$R_e´ =$ Distance between the phase image conductor and point P, in m.
$q_k =$ Load of the phase conductors, in C/m.
$x =$ Coordinate on the horizontal axis of point P, in m.
$y =$ Coordinate on the vertical axis of point P, in m.

Calculation of horizontal and vertical components

Based on Figure 2, the equations of the horizontal and vertical components of the electric field intensity of the HVAC overhead transmission line are derived. However, prior to the calculation, the following considerations must be taken:

1. The phase to neutral voltages are part of a balanced tree phase system, out of phase 120° electrical. A positive phase sequence is considered with phase b as a reference.

2. The real and imaginary components of the charges are considered.

Using the above considerations, the contributions of the electric field intensity due to the effect of the charge in each of the components (horizontal and vertical) are obtained.

The horizontal and vertical components are obtained by means of equations (1) and (2) respectively (Lunca, Ursache & Salceanu, 2017).

$$E_{x_k} = \sum_{k=1}^{N} E_C \left[\frac{x - x_k}{R_e^{\,2}} - \frac{x - x_k}{R_e^{\,\prime 2}} \right] \frac{V}{m} \quad (1)$$

For the vertical components, equation (2) is used.

$$E_{y_k} = -\sum_{k=1}^{N} E_C \left[\frac{y - y_k}{R_e^{\,2}} - \frac{y + y_k}{R_e^{\,\prime 2}} \right] \frac{V}{m} \quad (2)$$

Where:

$E_{x_k} =$ Horizontal component of electric field strength, in V/m.
$E_{y_k} =$ Vertical component of electric field strength, in V/m.
$N =$ Number of phases.
$E_C =$ Electric field effort at the surface of a conductor, in V/m.

The electric field effort on the surface of a phase conductor is obtained from equation (3) (Duncan & Malukutla, 2003).

$$E_C = \frac{q_k}{2\pi\varepsilon_0} \frac{V}{m} \quad (3)$$

ISSN 2410-3438

Where:

$\varepsilon_0 =$ Air permittivity $=8.854 \times 10^{-12}$, in $C^2/N \cdot m^2$.

The distance between the phase conductor and the measurement point P, is obtained by the equation (4) (Carsimamovic, Mujezinovic, Bajramovic, Turkovic, Kosarac & Stankovic, 2019).

$$R_e = \sqrt{(x - x_k)^2 + (y - y_k)^2} \text{ m} \quad (4)$$

The distance between the image phase conductor and the measurement point P, is obtained by the equation (5) (Carsimamovic, Mujezinovic, Bajramovic, Turkovic, Kosarac & Stankovic, 2019).

$$R_e' = \sqrt{(x - x_k)^2 + (y + y_k)^2} \text{ m} \quad (5)$$

Calculation of electric field strength

The total electric field intensity at the measurement point P is obtained by applying equation (6).

$$E_T = \sqrt{{E_{x_k}}^2 + {E_{y_k}}^2} \frac{\text{kV}}{\text{m}} \quad (6)$$

Where:

$E_T =$ Total magnitude of the electric field intensity at the measurement point P, in kV/m.

IEEE recommends that the electric field calculation be considered at 1 m above ground level (IEEE, 2002).

Case study

It is considered a 230 kV double circuit HVAC transmission line where you want to determine the intensity of the electric field at one meter above ground level, on a right of way of 80 m. Figure 3 shows the configuration of the transmission tower, the separation between the phases and their location above ground level. Table 2 shows the spatial coordinates of the phase conductor locations for the C-1 configuration. Table 3 shows the transmission line loads.

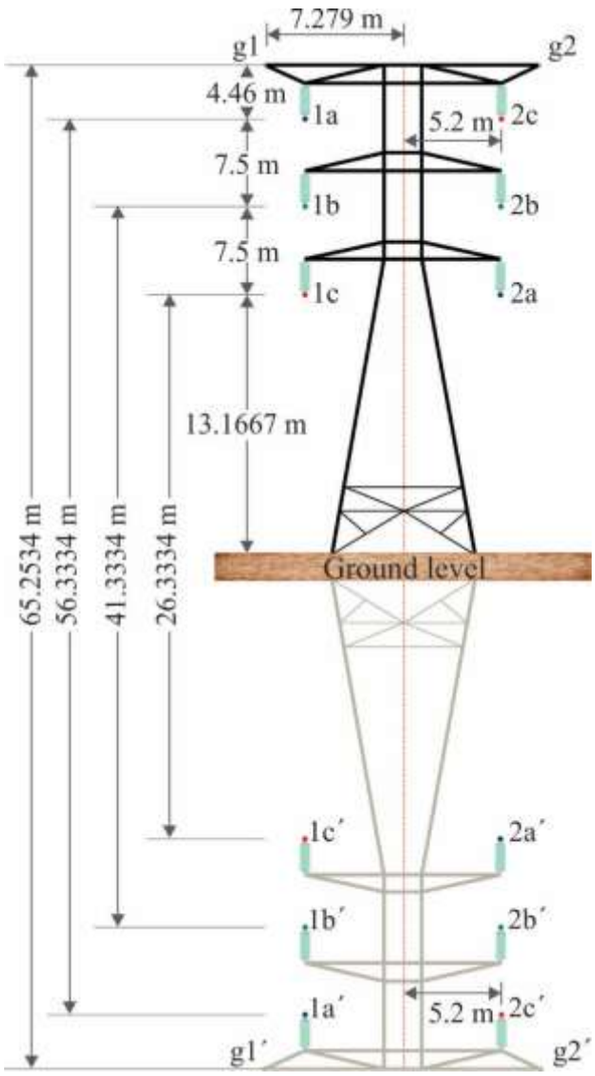

Figure 3 Profile of 230 kV HVAC double circuit transmission line
Source: Own elaboration

Phase	x_k	y_k
1a	-5.2 m	28.1667 m
1b	-5.2 m	20.6667 m
1c	-5.2 m	13.1667 m
2a	5.2 m	13.1667 m
2b	5.2 m	20.6667 m
2c	5.2 m	28.1667 m

Table 2 Spatial coordinates of the C-1 phase conductors of the double circuit transmission line
Source: Own elaboration

ISSN 2410-3438

Phase loading	Load in each phase, in C/m Polar shape	Rectangular shape
q_{1a}	$-661.801 \times 10^{-9} + 1.033 \times 10^{-6}$j	1.226 x10^{-6} ∠122.646
q_{1b}	1.193 x10^{-6} +1.142 x10^{-9} j	1.193 x10^{-6} ∠0.054
q_{1c}	–660.341 x10^{-9} –1.023 x10^{-6} j	1.217 x10^{-6} ∠–122.842
q_{2a}	–660.341 x10^{-9} +1.023 x10^{-6} j	1.217 x10^{-6} ∠122.842
q_{2b}	1.193 x10^{-6} –1.142 x10^{-9} j	1.193 x10^{-6} ∠–0.054
q_{2c}	–661.801 x10^{-9} –1.033 x10^{-6} j	1.226 x10^{-6} ∠–122.646

Table 3 Double circuit transmission line loads
Source: Own elaboration

Calculation of horizontal and vertical components

The calculation of the electric field effort is determined by means of equation (3).

$$E_C = \frac{\begin{bmatrix} -661.801\times10^{-9}+1.033\times10^{-6}\text{j} \\ 1.193\times10^{-6}+1.142\times10^{-9}\text{j} \\ -660.341\times10^{-9}-1.023\times10^{-6}\text{j} \\ -660.341\times10^{-9}+1.023\times10^{-6}\text{j} \\ 1.193\times10^{-6}-1.142\times10^{-9}\text{j} \\ -661.801\times10^{-9}-1.033\times10^{-6}\text{j} \end{bmatrix}}{(2\pi)(8.854\times10^{-12})} \text{ V} \times \frac{\text{kV}}{1000\text{ V}}$$

$$E_C = \begin{bmatrix} -11.8961 + 18.5686\text{j} \\ 21.4447 + 0.0205\text{j} \\ -11.8699 - 18.3889\text{j} \\ -11.8699 + 18.3889\text{j} \\ 21.4447 - 0.0205\text{j} \\ -11.8961 - 18.5686\text{j} \end{bmatrix} \text{ kV}$$

The distance from the phase conductor to the measurement point P is obtained, applying equation (4).

Distance from phase 1a, considering a point P (x=0, y=1).

$$R_{e1a} = \sqrt{(0-(-5.2))^2 + (1-28.167)^2}\text{ m}$$

$$R_{e1a} = 27.66\text{ m}$$

The distance from the phase conductor to the measurement point P (x=0, y=1), is obtained by applying equation (5).

$$R_{e'1a} = \sqrt{(0-(-5.2))^2 + (1+28.167)^2}\text{ m}$$

$$R_{e'1a} = 29.62\text{ m}$$

For the rest of the phase conductors and phase image conductors at point P (x=0, y=1) the results shown in Table 4.

Distance R_e	Distance R_e'
$R_{e1b} = 20.34$ m	$R_{e'1b} = 22.28$ m
$R_{e1c} = 13.23$ m	$R_{e'1c} = 15.09$ m
$R_{e2a} = 13.23$ m	$R_{e'2a} = 15.09$ m
$R_{e2b} = 20.34$ m	$R_{e'2b} = 22.28$ m
$R_{e2c} = 27.66$ m	$R_{e'2c} = 29.62$ m

Table 4 Distances R_e y R_e' to point P (x=0, y=1)

The calculation of the horizontal components of the electric field is performed using equation (1), for P (x=0, y=1).

$$\mathbf{Ex_0} = (E_{C1a})\left[\frac{x-x_{k1a}}{(R_{e1a})^2} - \frac{x-x_{k1a}}{(R_{e'1a})^2}\right]$$
$$+(E_{C1b})\left[\frac{x-x_{k1b}}{(R_{e1b})^2} - \frac{x-x_{k1b}}{(R_{e'1b})^2}\right]$$
$$+(E_{C1c})\left[\frac{x-x_{k1c}}{(R_{e1c})^2} - \frac{x-x_{k1c}}{(R_{e'1c})^2}\right]$$
$$+(E_{C1c})\left[\frac{x-x_{k1c}}{(R_{e1c})^2} - \frac{x-x_{k1c}}{(R_{e'1c})^2}\right]$$
$$+(E_{C2a})\left[\frac{x-x_{k2a}}{(R_{e2a})^2} - \frac{x-x_{k2a}}{(R_{e'2a})^2}\right]$$
$$+(E_{C2b})\left[\frac{x-x_{k2b}}{(R_{e2b})^2} - \frac{x-x_{k2b}}{(R_{e'2b})^2}\right]$$
$$+(E_{C2c})\left[\frac{x-x_{k2c}}{(R_{e2c})^2} - \frac{x-x_{k2c}}{(R_{e'2c})^2}\right]\frac{\text{kV}}{\text{m}}$$

$$\mathbf{Ex_0} = 0.00008 - 0.2203\text{j}\ \frac{\text{kV}}{\text{m}}$$

$$\mathbf{Ex_0} = \sqrt{(0.00008)^2 + (-0.2203\text{j})^2}\ \frac{\text{kV}}{\text{m}}$$

$$\mathbf{Ex_0} = 0.2203\ \frac{\text{kV}}{\text{m}}$$

The calculation of the vertical components of the electric field is performed using equation (2), for P (x=0, y=1).

$$\mathbf{Ey_0} = -1\ [(E_{C1a})\left[\frac{y-y_{k1a}}{(R_{e1a})^2} - \frac{y-y_{k1a}}{(R_{e'1a})^2}\right]$$
$$+(E_{C1b})\left[\frac{y-y_{k1b}}{(R_{e1b})^2} - \frac{y-y_{k1b}}{(R_{e'1b})^2}\right]$$
$$+(E_{C1c})\left[\frac{y-y_{k1c}}{(R_{e1c})^2} - \frac{y-y_{k1c}}{(R_{e'1c})^2}\right]$$
$$+(E_{C1c})\left[\frac{y-x_{k1c}}{(R_{e1c})^2} - \frac{y-y_{k1c}}{(R_{e'1c})^2}\right]$$

$$+(E_{C2a})\left[\frac{y-y_{k2a}}{(R_{e2a})^2}-\frac{y-y_{k2a}}{(R_{e'2a})^2}\right]$$

$$+(E_{C2b})\left[\frac{y-y_{k2b}}{(R_{e2b})^2}-\frac{y-y_{k2b}}{(R_{e'2b})^2}\right]$$

$$+(E_{C2c})\left[\frac{y-y_{k2c}}{(R_{e2c})^2}-\frac{y-y_{k2c}}{(R_{e'2c})^2}\right]\frac{kV}{m}$$

$$\mathbf{Ey_0} = -0.8536 + 0j\ \frac{kV}{m}$$

$$\mathbf{Ey_0} = \sqrt{(-0.8536)^2 + (0j)^2}\ \frac{kV}{m}$$

$$\mathbf{Ey_0} = 0.8536\ \frac{kV}{m}$$

Calculation of electric field strength

Finally, the total intensity of the electric field is calculated at the measurement point P (x= 0, y= 1), using equation (6).

$$E_{T0} = \sqrt{(0.2203\ )^2+(0.8536)^2}\ \frac{kV}{m}$$

$$E_{T0} = 0.8815\ \frac{kV}{m}$$

Table 5 shows the results obtained from the total intensity of the electric field on the right of way, using intervals of 10 m of the right of way.

Coordinates	Electric field intensity, in kV/m
P (x= 0, y= 1)	$E_{T0} = 0.8815$
P (x= 10, y= 1)	$E_{T10} = 1.1475$
P (x= 20, y= 1)	$E_{T20} = 0.3070$
P (x= 30, y= 1)	$E_{T30} = 0.0610$
P (x= 40, y= 1)	$E_{T40} = 0.0406$

Table 5 Electric field intensity on the right of way of the transmission line

In Figure 4, the plotted results of the electric field intensity on the right of way of the 230 kV double circuit transmission line.

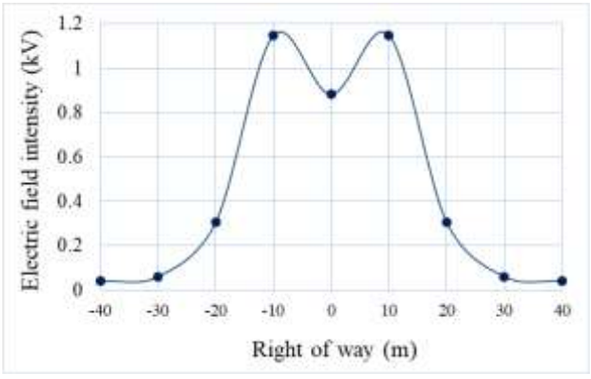

Figure 4 Electric field intensity of C-1 from transmission line

Figure 4 shows that for the transmission line under study, the maximum electric field intensity is 1.1475 kV/m, which is lower than the maximum limit recommended by (Sarma, 2000).

Results

To obtain a validation of the methodology presented to calculate the intensity of the electric field, a simulation of the transmission line under study is carried out, for this the FACE software was used (FACE, 2019).

Table 6 and Figure 5 show the comparison of the results obtained between the methodology presented and the validation of the FACE software.

Electric field strength	
Methodology, in kV	FACE, in kV
$E_{T0} = 0.8815$	$E_{T0} = 0.8815$
$E_{T10} = 1.1475$	$E_{T10} = 1.1475$
$E_{T20} = 0.3070$	$E_{T20} = 0.3070$
$E_{T30} = 0.0610$	$E_{T30} = 0.0610$
$E_{T40} = 0.0406$	$E_{T40} = 0.0406$

Table 6 Comparison of the results obtained between the methodology and the FACE software

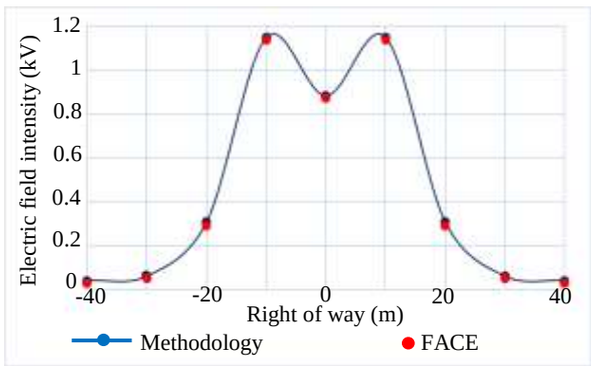

Figure 5 Comparison of the results obtained between the methodology and the FACE software

Comparing the results, a percentage difference of 2% is present between the methodology and the FACE software.

Optimization of the phases of the circuits in the electric field intensity

For the optimization of the phases in the transmission line, 2 configurations are considered (C-2 and C-3), which are presented in Tables 7 and 8 respectively. This will allow to evaluate the behavior of the electric field intensity.

Table 7 shows the coordinates of the C-2 phase conductors of the transmission line.

Phase	x_k	y_k
1a	-5.2 m	28.1667 m
1b	-5.2 m	20.6667 m
1c	-5.2 m	13.1667 m
2c	5.2 m	28.1667 m
2b	5.2 m	20.6667 m
2a	5.2 m	13.1667 m

Table 7 Coordinates of the phase conductors of C-2 of the transmission line

Performing the procedure of the methodology with configuration presented in Table 7, the results of the electric field intensity on the right of way shown in Figure 6 are obtained.

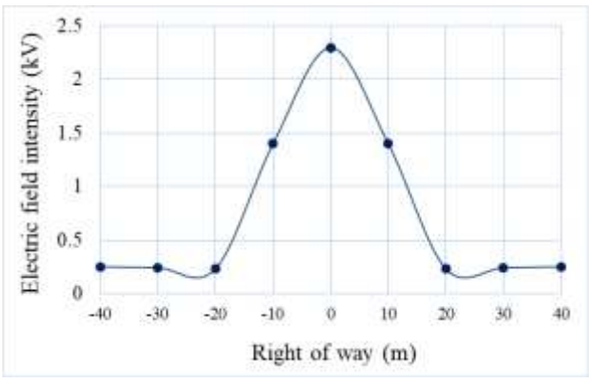

Figure 6 Electric field intensity of C-2 from HVAC 230 kV double circuit transmission line

Table 8 shows the coordinated of the C-3 phase conductors of the transmission line.

Phase	x_k	y_k
1c	-5.2 m	13.1667 m
1a	-5.2 m	28.1667 m
1b	-5.2 m	20.6667 m
2a	5.2 m	13.1667 m
2b	5.2 m	20.6667 m
2c	5.2 m	28.1667 m

Table 8 Coordinates of the phase conductors of C-3 of the transmission line

Carry out the previous procedure with the configuration shown in Table 8, the results of the electric field intensity on the right of way shown in Figure 7 are obtained.

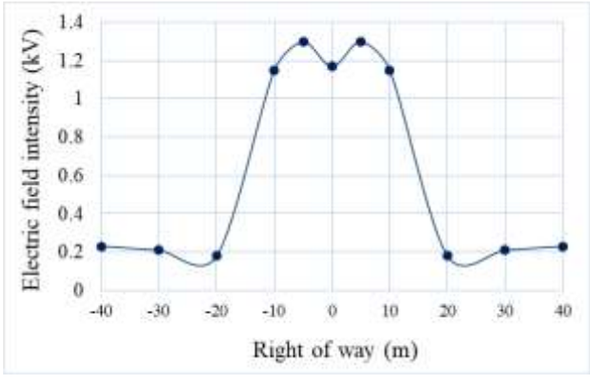

Figure 7 Electric field intensity of C-3 from HVAC 230 kV double circuit transmission line

Based on the results obtained, a better behavior of the electric field intensity is observed considering the C-1 configuration, with a better performance of 11.73% compared to C-2 and 50.53% compared to C-3.

Conclusions

The following points are concluded from the article made:

- A reference methodology is presented, which contains the necessary steps to perform the calculation of the electric field intensity on the right of way of HVAC overhead transmission lines.
- The methodology presented may be applied in transmission lines of 1 to n circuits, admitting the different nominal voltages of the HVAC lines.
- By optimizing the phases of the transmission line circuits, the most efficient configuration for obtaining the electric field intensity is determined.
- The electric field intensity profile of the 230 kV HVAC double circuit transmission line was validated with the FACE software, with which a difference of 2% is obtained.
- In future works, the methodology presented may be applied avoiding the use of commercial programs, since this methodology has been successfully validated.

References

Adel, Z. & Dein, E. (2013). Effect of the variation pf the charge distribution along multi-overhead transmission lines' conductors on the calculation method of ground surface electric field.

ISSN 2410-3438

Aguilar, J. Cisneros, L. Padilla, J & Vergara, J. (2020). Methodology to calculate the density of the magnetic field generated in overhead transmission lines in HVDC applying a two-dimensional analysis of parallel poles above ground level. Journal – Democratic Republic of Congo.

Carsimamovic, A. Mujezinovic, A. Bajramovic, Z. Turkovic, I. Kosarac, M. & Stankovic, K. (2019). Origin and mitigation of increased electric fields at high voltage transmission line conductors.

Duncan, J. & Malukutla, S. (2003). Sistemas de potencia.

Duncan, J. & Malukutla, S. (1993). Power system analysis.

FACE. (2019). Field and corona effects, Manitoba hydro international. Canada.

Grainger, J. & Stevenson, W. (1996). Análisis de sistemas eléctricos de potencia.

IEEE. (2002). IEEE STD C95.6 Safety levels with respect to human exposure to electromagnetic fields, 0-3 kHz.

IEC. (2014). IEC 62681 Electromagnetic performance of high voltage direct current (HVDC) overhead transmission lines.

Lunca, E. Ursache, S. & Salceanu, A. (2017). Computation and Analysis of the Extremely Low Frequency Electric and Magnetic Fields Generated by Tow Designs of 400 kV Overhead Transmission Lines.

Ortiz, L. (2007). Estudio de campos eléctricos y magnéticos de la línea de transmisión de 220 kV, Pan de Azúcar-Andacollo. Santiago de Chile.

Samy, M. Radwan, R. & Akef, S. (2017). Calculation of electric fields underneath and on conductor surfaces of ultra high voltage transmission lines.

Sarma, Maruvada, P. (2000). Corona performance of high-voltage transmission lines. Canada.

Ukil, A. (2015). Theoretical analysis of tuned HVAC line for low loss long distance bulk power transmission.

ISSN 2410-3438

Article **Journal of Quantitative and Statistical Analysis**
December, 2020 Vol.7 No.21 9-17

Laboratory data statistical analysis from CECCS' patients with or without SARS-CoV-2 (COVID-19)

Análisis estadístico de datos de laboratorio de pacientes del CECCS con o sin SARS-CoV-2 (COVID-19)

YAÑEZ-VARGAS Israel†*, DOÑATE-ÁLVAREZ Andrea, QUINTANILLA-DOMINGEZ Joel and AGUILERA-GONZÁLEZ Gabriel

Universidad Politécnica de Juventino Rosas, Departamento de Ingeniería en Redes y Telecomunicaciones.

ID 1st Author: *Juan Israel Yañez-Vargas* / **ORC ID:** 0000-0001-5749-8442, **CVU CONACYT- ID:** 295711

ID 1st Coauthor: *Andrea Abigail Doñate-Álvarez* / **ORC ID:** 0000-0003-4005-8533

ID 2nd Coauthor: *Joel Quintanilla-Domínguez*/ **ORC ID** 0000-0003-2442-2032, **CVU CONACYT- ID:** 295711

ID 3rd Coauthor: *José Aguilera-González*/ **ORC ID:** 0000-0002-4160-448X, **CVU CONACYT- ID:** 329447

DOI: 10.35429/JQSA.2020.21.7.9.17 Received September 05, 2020; Accepted December 01, 2020

Abstract

The increase in the number of COVID-19 cases in Mexico has caused an important effort in the analysis of the virus, due to the above, a statistical study of laboratory data of 109 patients from the State Center for Critical Care of Salamanca (CECCS) with or without COVID-19, whose purpose is to analyze in more detail the disease and the reactions in patients. First, a classification was made in men and women, then positive, negative, healthy and deceased patients. It is important to mention that a data cleaning was carried out, in addition to information filling using the mean of the laboratory values, then the clinical data were normalized from 0 to 1, to obtain the BMI of the patients, box plots and graphs days to days of hospitalization with a sample of patients.

COVID-19, Clinical laboratory data, Statistical analysis

Resumen

El incremento en número en casos COVID-19 en México ha provocado un esfuerzo importante en el análisis del virus, debido a lo anterior, se ha propuesto un estudio estadístico de datos de laboratorio de 109 pacientes del Centro Estatal de Cuidados Críticos de Salamanca (CECCS) con o sin COVID-19, cuyo propósito es analizar más a detalle la enfermedad y las reacciones en los y las pacientes. Primero, se realizó una clasificación en hombres y mujeres, posteriormente pacientes positivos, negativos, pacientes sanos y con defunción. Es importante mencionar que se realizó una limpieza de los datos, además de un llenado de información usando la media de los valores de los laboratorios, posteriormente se normalizaron los datos clínicos de 0 a 1, para obtener las gráficas de la clasificación e IMC de los pacientes, diagramas de caja y gráficas de los días de hospitalización de una muestra de pacientes.

COVID-19, Datos clínicos de laboratorio, Estudio estadístico

Citation: YAÑEZ-VARGAS Israel, DOÑATE-ÁLVAREZ Andrea, QUINTANILLA-DOMINGEZ Joel and AGUILERA-GONZÁLEZ Gabriel. Laboratory data statistical analysis from CECCS' patients with or without SARS-CoV-2 (COVID-19). Journal of Quantitative and Statistical Analysis. 2020. 7-21: 9-17

* Correspondence to Author (e-mail: jyanez_ptc@upjr.edu.mx)
† Researcher contributing as first author.

Article Journal of Quantitative and Statistical Analysis
December, 2020 Vol.7 No.21 9-17

1. Introduction

In December 2019, a new type of coronavirus originated in the city of Wuhan, China. The scientific family called it Severe Acute Respiratory Syndrome (SARS-CoV-2), which is the cause of COVID-19 that today has become official as a global pandemic (Coronavirus disease (COVID-19), 2020).

Given the great challenge of the scientific community in the knowledge of COVID-19, multiple studies have been carried out for its detection and complete analysis since the behavior of COVID-19 in each country or region will depend on many factors, such as susceptibility to diseases, the most common diseases, age, weight, weather and other factors.

The Federal Health Secretariat of Mexico, through the General Directorate of Epidemiology, reported that, as of December 15, 2020, more than 73 million confirmed cases have been recorded worldwide, in addition to more than 1.6 million deaths from COVID-19. In Mexico, there are currently more than 1.4 million confirmed cases, while there are around 114 thousand deaths (Coronavirus - gob.mx, 2020).

Given the above, it is necessary to know the action of the virus in humans, for which it is intended to carry out a statistical study based on clinical laboratory data obtained from the State Center for Critical Care of Salamanca (CECCS), which is a hospital of third level that was converted into the first hospital dedicated to COVID-19 in the state of Guanajuato and is located in the city of Salamanca (Conversion of the CECCS to a COVID-19 center, 2020).

From all the information obtained and processed, it will be possible to understand the severity of the patient, the condition and know the behavior of the virus in the human body. Carrying out a statistical study or having a data analysis will allow to give greater validity to some affirmations made about the virus, in addition to making better decisions based on mathematical analysis with real data.The branches of engineering and medicine have become very involved in recent years, where statistical studies are continuously carried out in order to learn more about phenomena of global importance, therefore, derived from the global pandemic of COVID-19, the efforts in all areas to learn more about the virus.

In the study by K. Liu et al. (2020, p. 1027) showed the results of processing the epidemiological history data, analyzing the clinical characteristics, treatments and the prognosis of 137 patients admitted with COVID-19, they presented the results on the most recurrent symptoms, the most susceptible ages and chest X-ray images of each patient.

According to a new study where a statistical investigation was carried out on clinical and biochemical data of 12 patients infected with COVID-19, to know the changes in the patient through the use of certain medications, likewise a study based on images was added X-ray and tomography (Y. Liu et al., 2020, p. 372).

(Ng et al., 2020) in their research article, they describe 21 patients confirmed as positive for COVID-19, they underwent X-ray and tomography studies to know their evolution, in addition to showing statistical study of data personal symptoms and some clinical results.

In the study by Yun et al. (2020, 96 p.) Carry out a study with clinical data of nucleic acid and blood from 2510 patients infected with COVID-19, Influenza A and Influenza B, showing statistically comparisons of the changes in each of the laboratory studies.

Zhang et al. (2020, p. 1736) presented in their study an analysis of data from 140 patients with SARS-CoV-2 in which information on demographic data, allergies, clinical manifestations, comorbidities, and laboratory data is grouped for subsequent mathematical analysis.

All previous studies and most of those registered worldwide seek to have a broader knowledge of the behavior of the virus in both men and women, but the existence of documentation for Mexico is much less and if it is established that for patients from the state of Guanajuato and admitted to third-level hospitals is more scarce, makes this research of utmost importance to know the evolution of the virus and patient in a sample of the population infected with COVID-19 of Guanajuato.

ISSN 2410-3438

2. Material and methods

When the patient is admitted to the tertiary level hospital, a data collection is carried out which includes name, age, weight and comorbidities if they have them, to later be admitted to intensive care.

The data to be analyzed correspond to 109 patients from the CECCS hospital, which is a third-level center located in the city of Salamanca, Guanajuato, they were admitted from March 24 to October 20, 2020.

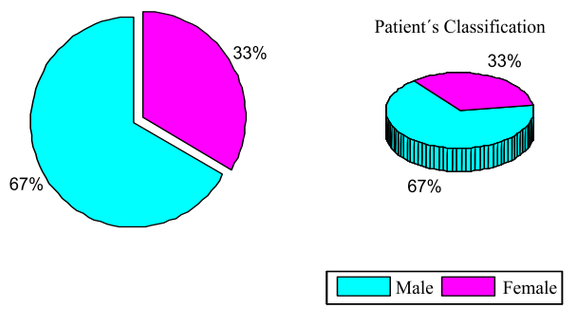

Figure 1 Total patients admitted to the CECCS
Source: Own [Matlab]

Figure 1 shows a diagram of the division of patients admitted to the hospital, of which there are 73 men and 36 women.

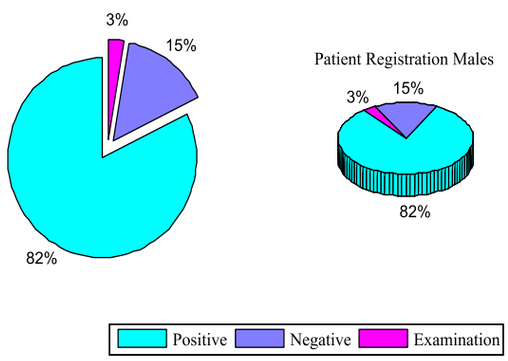

Figure 2 Men admitted to the CECCS
Source: Own [Matlab]

Likewise, in Figure 2 of the 73 men admitted to the hospital, there are 60 patients who tested positive for the Polymerase Chain Reaction (PCR) test for COVID-19, which is the most used due to its great reliability. in the result, while 11 people were negative to the test, leaving 2 people still in observation or waiting for the result of the PCR test (Dra. Celia M. Alpuche Aranda, 2020).

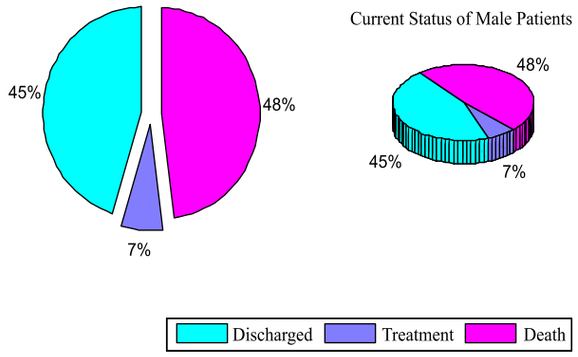

Figure 3 Current status of male patients in the CECCS
Source: Own [Matlab]

From the data shown above, a relationship was obtained of those patients who are still hospitalized with treatment, those who died and those who lived. Figure 3 gives a graphic explanation of the percentage of 109 patients who died, having a high percentage for the number of patients admitted.

In the case of the 36 women who were admitted to the hospital, Figure 4 shows in detail the case of the patients who were positive, negative and who have not yet obtained the result of their PCR test.

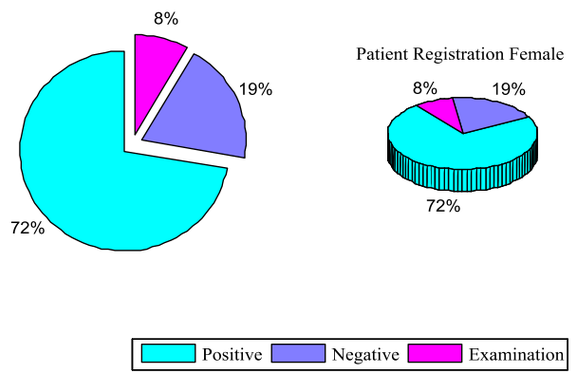

Figure 4 Registry of female patients with their PCR result
Source: Own [Matlab]

Finally, Figure 5 shows results of female patients and their status in the hospital, showing percentages of patients discharged, in death and treatment.

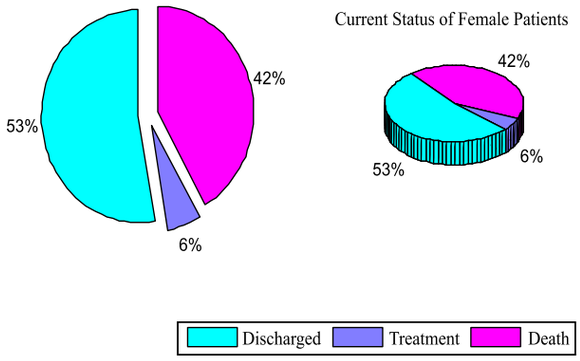

Figure 5 Current status of female patients
Source: Own [Matlab]

As mentioned above, when patients are admitted to the CECCS, measurements of the height and weight of the patients are carried out, to later carry out a study of the Body Mass Index (BMI), either to learn more about the health status of the person and the amount of medication to be prescribed.

Figure 6 describes the BMI of female patients, where it should be remembered that from a BMI value of 25 people become overweight, where it is possible to notice that most women are overweight and some are overweight. grade III obesity.

.

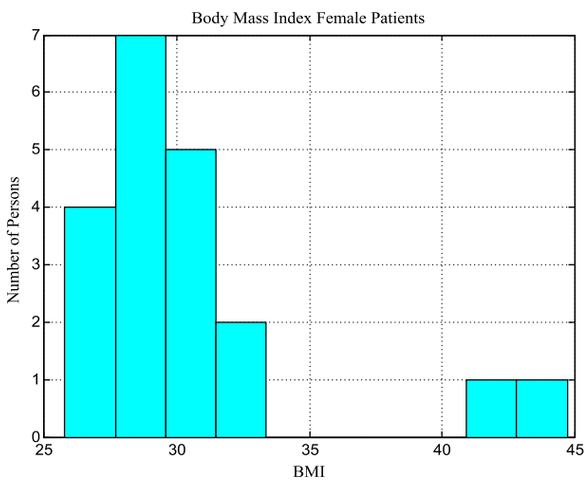

Figure 6 BMI of female patients
Source: Own [Matlab]

In the case of Figure 7, the BMI of men is shown, in which an important difference can be noticed with respect to the graph of women, since men are more overweight than women, despite the fact that the greater cases of overweight occurred in women.

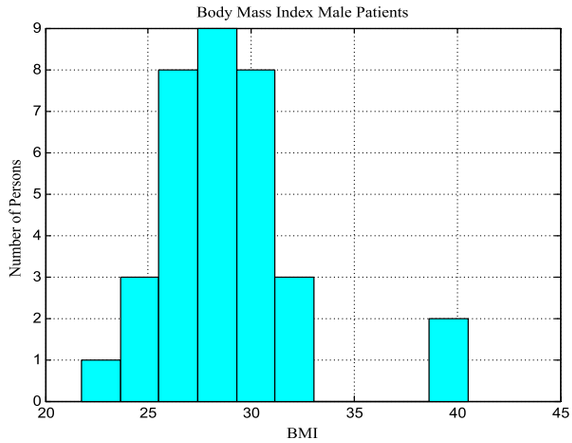

Figure 7 BMI of male patients
Source: Own [Matlab]

3. Clinical laboratory data

Different laboratory tests are performed daily from the first day to the last day of the patients' stay. There were 39 different laboratories that were obtained, although not all patients have sufficient data to be able to process them, so it was decided to perform a data cleaning in which it was reduced to 28 laboratories that are mentioned below: Glucose, Urea, Nitrogen Ureic, Creatinine, Total Proteins, Albumin, Globulin, A / G Ratio, Alanine Amino Transferase, Aspartate Amino Transferase, Total Bilirubin, Direct Bilirubin, Indirect Bilirubin, Lactic Dehydrogenase, Creatine-Phosphokinase, Chlorine, Potassium, Sodium, Time, Cytometry Prothrombin, Thromboplastin Time, Fibrinogen, Procalcitonin, Calcium, Phosphorus, Alkaline Phosphate, Magnesium, C. Reactive Protein (Pagana & Pagana, 2015)

4. Methodology

To carry out the statistical study of the CECCS data, a general block diagram was made, which is shown in Figure 8, each of the blocks has been described later. The data collection block corresponds to the collection of information contained in the hospital database, the information includes the graphs described in section 2, in addition to the data described in section 3. In blocks 2 and 3, the an analysis of the stored information, either to rule out errors, in addition to dividing the information into men and women, it is important to mention that several patients have missing data, for which the technique of imputation of the mean was used to add values missing in each laboratory of incomplete patients (Devore, 2012), (Gutierrez & Vladimirovna, 2014).

ISSN 2410-3438

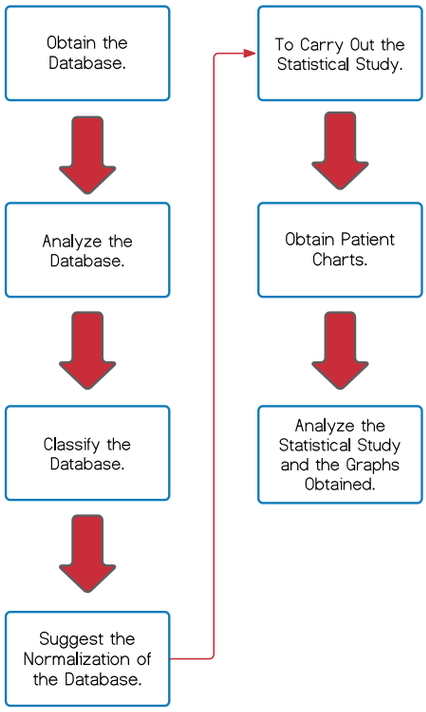

Figure 8 General block diagram
Own Source

Each one of the 28 laboratory studies in the database of each patient represents a vector of values, therefore, each vector is independent of each other, due to the above because each laboratory handles different representations measurement requires standardization of each of the data, given the above, a normalization from 0 to 1 was carried out, from the minimum and maximum values of each of the vectors independently (Gonzalez & Woods, 2008).

The fifth block is the realization of the statistical part, obtaining information on the minimum, maximum, mean, median values, the box and whisker diagrams, statistics of the behavior of the day-to-day laboratories and other extra statistics that were used Throughout the study, block six is only the display of statistics, while block seven is a study of the results obtained in the graphs and their subsequent interpretation (Devore, 2012), (Gutierrez & Vladimirovna, 2014).

5. Results

The statistical study and its interpretation will allow to know a little more about the virus and the behavior in the Guanajuato population, before which multiple graphs were made for both women and men.

Figure 9 represents the box and whisker diagrams of each of the laboratories of the women who were discharged from CECCS, the idea is to represent the averages in the changes in each laboratory, as well as their behavior during the different days. that lasted hospitalized.

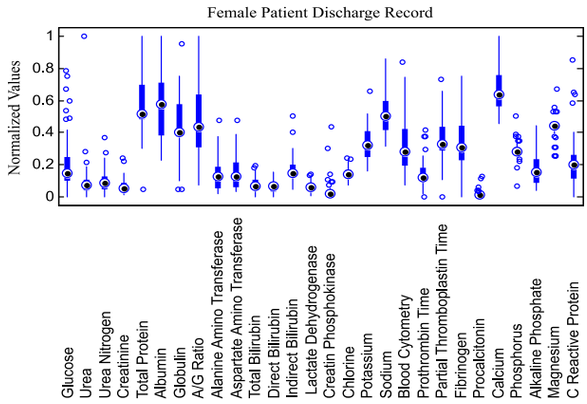

Figure 9 Laboratories of women registered
Source: Own [Matlab]

Each one of the graphs represents a sample of all the laboratories obtained from the women throughout the different days that they were admitted to the hospital.

In the case of Figure 10, the same graph is shown, but for female patients who died during their stay in the hospital, where multiple changes are observed compared to Figure 9, having higher mean values, higher variances , higher atypical values and in some cases very abrupt changes, such as in Glucose, Urea, Ureic Nitrogen and Total Proteins, as well as in the Partial Thromboplastin Time and C-Reactive Protein.

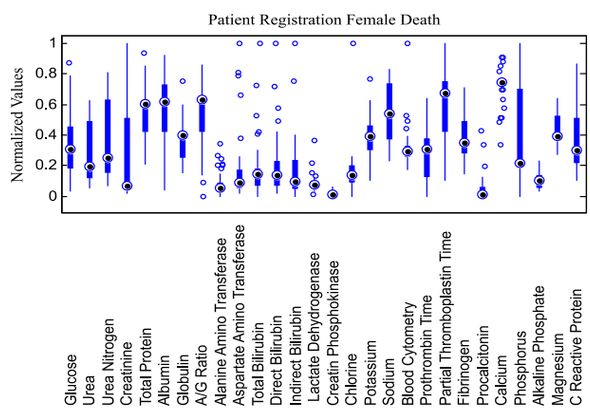

Figure 10 Laboratories of women who died
Source: Own [Matlab]

The graph in Figure 11 describes the case of the men who were discharged, where the diagrams of some laboratories with trends similar to those of the women who lived can be observed and their result is represented in Figure 9. Let us remember that the men's data is a sample of all the patients admitted to the CECCS, in which this sample of previously selected patients was saved in a database with all the laboratories obtained daily, to finally obtain the graphs of diagrams of boxes and whiskers shown.

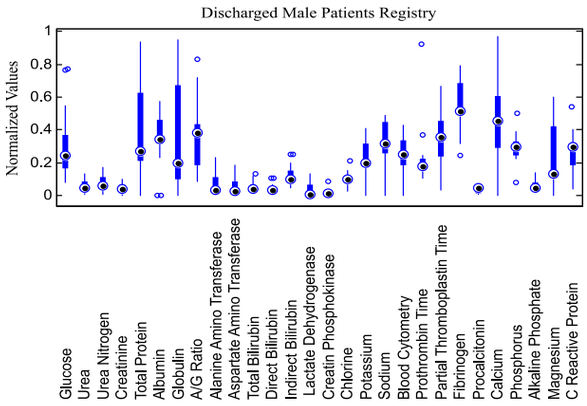

Figure 11 Labs of men discharged
Source: Own [Matlab])

Figure 12 shows the diagrams of the men who died, the graph shows greater changes in laboratories of C-Reactive Protein, Magnesium, Fibrinogen, Hematic Cytometry, Sodium, Glucose, Urea, Ureic Nitrogen, in addition to having more values atypical.

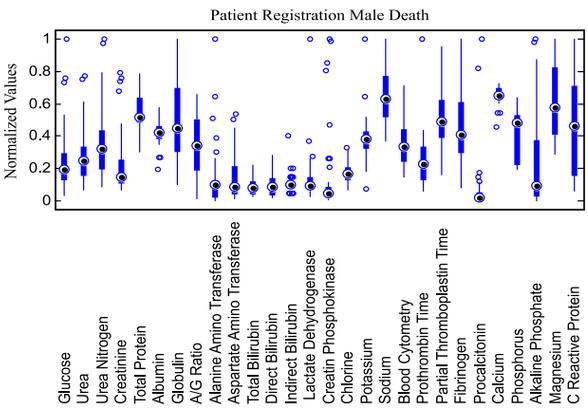

Figure 12 Laboratories of Men who died
Source: Own [Matlab]

From the previous graphs, certain relevant information can be observed, since, in the case of women, on average, they die with higher values in the different laboratories and also have wider variances, but it is not yet a strong conclusion Therefore, more studies are required, before that, box and whisker diagrams were made to compare the laboratories of a man and a woman who lived and died.

Figure 13 describes the results of a woman, named as patient 14, who was discharged after 31 days, where lower outliers are observed and the variances are lower, as well as the means are lower.

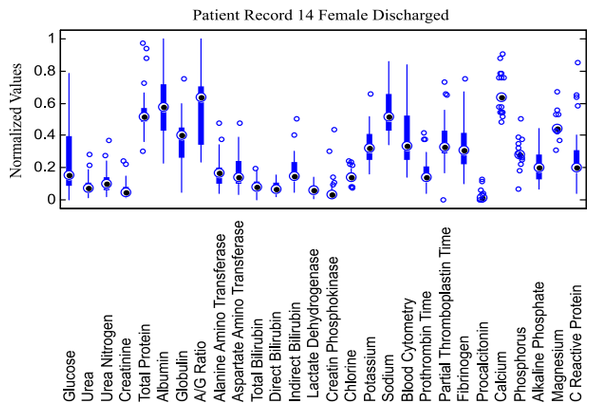

Figure 13 Laboratories for women discharged
Source: Own [Matlab]

Unlike the previous Figure, Figure 14 shows the results of patient 2, who died, in which there are more outliers, the mean is higher, as well as the variance in most laboratories.

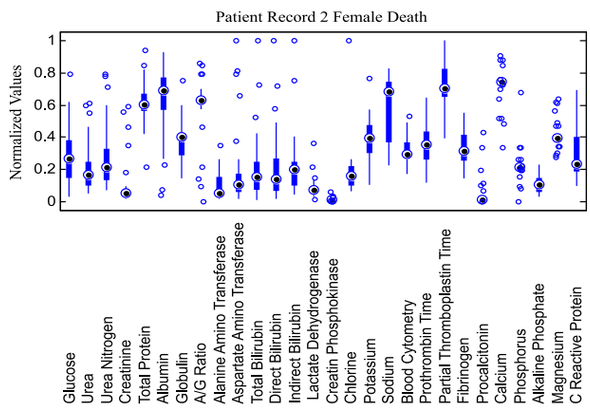

Figure 14 Laboratories of Woman who died
Source: Own [Matlab]

Figure 15 describes the results of a man, named as patient 16, who was discharged after 14 days, where lower outliers are observed and the variances are lower, as well as the means are lower.

ISSN 2410-3438

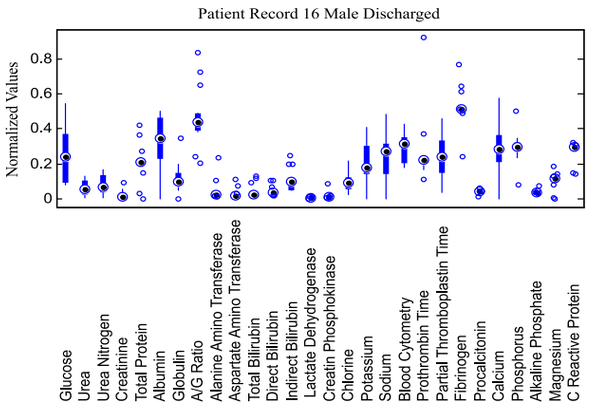

Figure 15 Laboratories of Man discharged
Source: Own [Matlab]

Compared to the previous Figure, Figure 16 shows the results of patient 17, who died after 13 days, in which there are more outliers, the mean is higher, as well as the variance in most laboratories, It is important to notice the strongest changes in Glucose, Urea, Ureic Nitrogen, Creatine-Phosphokinase, Sodium, Fibrinogen, Magnesium and C-Reactive Protein.

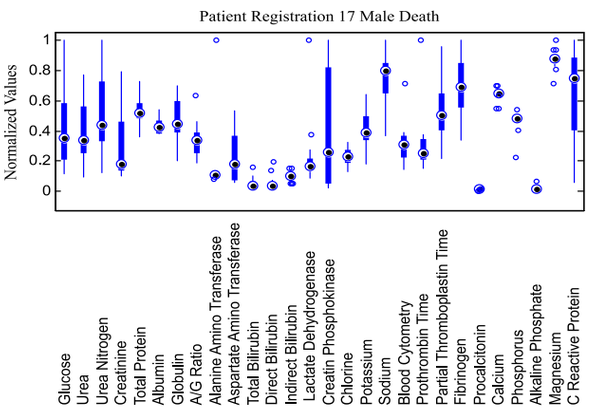

Figure 16 Laboratories of Man who died
Source: Own [Matlab]

The sample of 4 patients chosen to obtain their previous statistics describes the averages, variances, minimums and maximums of each laboratory. Likewise, graphs of the laboratory's day-to-day are added, in order to analyze the behavior of patients during their stay in the hospital.

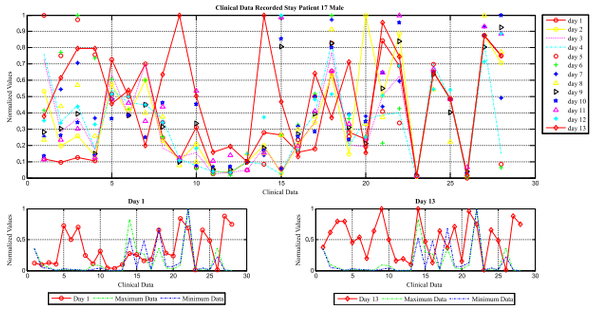

Figure 17 Patient behavior 17
Source: Own [Matlab]

The diagrams in Figure 17 show the laboratories obtained day by day during their stay, remembering that the patient died after 13 days, the Figure shows 3 graphs, the first one describes large variations in the values, the second graph (bottom left) represents the laboratory values of the first day in the hospital, likewise the minimum and maximum normal values of each laboratory are added, the third graph (lower right) shows the laboratory values of the last day of hospital stay, the values they are very high compared to the first day of stay.

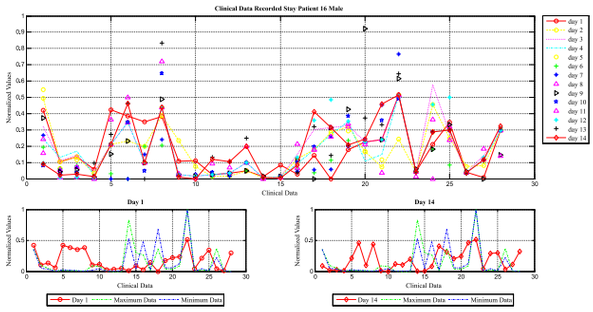

Figure 18 Patient behavior 16
Source: Own [Matlab]

For Figure 18 there are 3 graphs, the largest shows the behavior of patient 16 throughout the 14 days of stay, the lower left graph explains the first day of stay, the graph on the right side shows the last day of stay.

As in the previous figures, 3 graphs of patient 2 who died are shown, in Figure 19 it is possible to note the changes in values of each laboratory on the different days, showing the difference between the first day and the last day.

ISSN 2410-3438

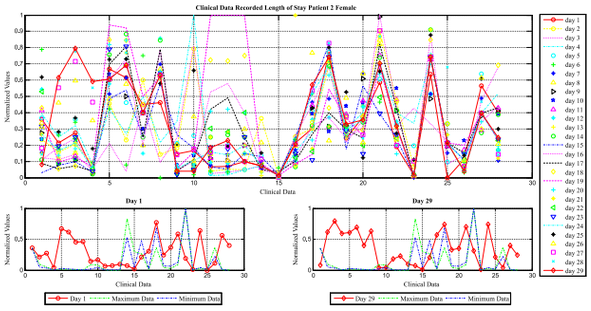

Figure 19 Behavior of patient 2
Source: Own [Matlab]

For patient 14 who was discharged after 31 days it is possible to analyze the laboratory results of the different days in Figure 20, then it shows a stabilization of the data at the end of her stay.

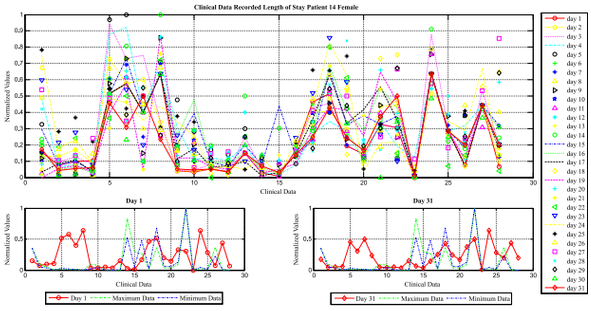

Figure 20 Behavior of patient 14
Source: Own [Matlab]

6. Conclusions

In this article, a statistical analysis of the patients admitted to the CECCS in Salamanca was carried out, which includes patients with COVID-19 and not COVID-19 from the state of Guanajuato, the graphs show trends similar to those observed at the national and international level .

The patients admitted were those with greater severity in the state, likewise, they were patients who were more overweight in both men and women, it is also important to mention that there were higher admissions in men than in women, in addition to the fact that more men were the who passed away.

From the sample of patients taken and derived from the statistics, it is also possible to analyze that women have greater resistance according to the graphs to COVID-19 than men and even have higher values in multiple laboratory results.

The statistics analyzed will make it possible to carry out a comparative study of the drugs supplied and their evolution during their stay, in addition to knowing the evolution of the patient, the use of ventilators and even making estimates of behavior or prevention of deaths in patients.

Acknowledgments

The authors would like to thank the State Center for Critical Care of Salamanca (CECCS), the doctor Dr. Cesar Centeno Fosado and the head of nurses Liliana Yañez Vargas for their support in preparing the article and providing the database.

References

Conversión del CECCS a centro COVID-19. *(2020, 7 abril). Centro Estatal de Cuidados Críticos de Salamanca. https://boletines.guanajuato.gob.mx/2020/04/07/ssg-reconvierte-centro-estatal-de-cuidados-criticos-en-unidad-especializada-para-atencion-de-pacientes-con-covid-19/*

Coronavirus – *gob.mx*. (2020, 14 diciembre). https://coronavirus.gob.mx/

Coronavirus disease (COVID-19). (2020, 14 diciembre). Coronavirus disease (COVID-19) pandemic. https://www.who.int/emergencies/diseases/novel-coronavirus-2019

Devore, J., 2012. Probability And Statistics For Engineering And The Sciences. 8th ed. Australia: Brooks/Cole, pp.28-38.

Dra. Celia M. Alpuche Aranda. (2020, junio). *Informe Técnico Reunión De Expertos Sobre Uso De Pruebas De Laboratorio Para Identificar SARS-COV-2* (N.º 1). Subsecretaría De Prevención Y Promoción De La Salud Dirección General De Epidemiología. https://coronavirus.gob.mx/wp-content/uploads/2020/06/Docto_InfTec-SARS-COV2_26jun2020.pdf

Gonzalez, R. C., & Woods, R. E. (2008). *Digital Image Processing* (3ª ed.). USA: Pearson/Prentice Hall.

Gutiérrez González, E. and Vladimirovna Panteleeva, O., 2014. Probabilidad Y Estadística. 1st ed. México: Grupo Editorial Patria, pp.287-323.

Liu, K., Fang, Y.-Y., Deng, Y., Liu, W., Wang, M.-F., Ma, J.-P., Xiao, W., Wang, Y.-N., Zhong, M.-H., Li, C.-H., Li, G.-C., & Liu, H.-G. (2020). Clinical characteristics of novel coronavirus cases in tertiary hospitals in Hubei Province. *Chinese Medical Journal*, *133*(9), 1025-1031. https://doi.org/10.1097/cm9.0000000000000744

Liu, Y., Yang, Y., Zhang, C., Huang, F., Wang, F., Yuan, J., Wang, Z., Li, J., Li, J., Feng, C., Zhang, Z., Wang, L., Peng, L., Chen, L., Qin, Y., Zhao, D., Tan, S., Yin, L., Xu, J., … Liu, L. (2020). Clinical and biochemical indexes from 2019-nCoV infected patients linked to viral loads and lung injury. *Science China Life Sciences*, *63*(3), 364-374. https://doi.org/10.1007/s11427-020-1643-8

Ng, M.-Y., Lee, E. Y. P., Yang, J., Yang, F., Li, X., Wang, H., Lui, M. M.-, Lo, C. S.-Y., Leung, B., Khong, P.-L., Hui, C. K.-M., Yuen, K.-, & Kuo, M. D. (2020). Imaging Profile of the COVID-19 Infection: Radiologic Findings and Literature Review. *Radiology: Cardiothoracic Imaging*, *2*(1), e200034. https://doi.org/10.1148/ryct.2020200034

Pagana, K., & Pagana, T. (2015). *Laboratorio clínico: Indicaciones e interpretación de resultados* (1.ª ed.). Editorial El Manual Moderno.

Yun, H., Sun, Z., Wu, J., Tang, A., Hu, M., & Xiang, Z. (2020). Laboratory data analysis of novel coronavirus (COVID-19) screening in 2510 patients. *Clinica Chimica Acta*, *507*, 94-97. https://doi.org/10.1016/j.cca.2020.04.018

Zhang, J.-, Dong, X., Cao, Y.-, Yuan, Y.-, Yang, Y.-, Yan, Y.-, Akdis, C. A., & Gao, Y.-. (2020). Clinical characteristics of 140 patients infected with SARS-CoV-2 in Wuhan, China. *Allergy*, *75*(7), 1730-1741. https://doi.org/10.1111/all.14238

ISSN 2410-3438

Article **Journal of Quantitative and Statistical Analysis**
December, 2020 Vol.7 No.21 18-27

Analysis and automatic segmentation of images for lungs regions extraction in X-ray chest

Analisis y segmentación automática de imágenes para extraer las regiones pulmonares en radiografías de torax

QUINTANILLA-DOMÍNGUEZ, Joel†*, YAÑEZ-VARGAS, Juan Israel, BUTANDA-SERRANO, Miriam and SÁNCHEZ-TORRECITAS, Enrique

Universidad Politécnica de Juventino Rosas, Dept. Engineering in Networks and Telecommunications & Master in Engineering-Intelligent Systems, Mexico.

ID 1st Author: *Joel, Quintanilla-Domínguez* / **ORC ID:** 0000-0003-2442-2032

ID 1st Coauthor: *Juan, Yañez-Vargas* / **ORC ID:** 0000-0001-5749-8442

ID 2nd Coauthor: *Miriam, Butanda-Serrano* / **ORC ID:** 0000-0003-1405-0204

ID 3rd Coauthor: *Enrique, Sánchez-Torrecitas* / **ORC ID:** 0000-0002-5395-6749

DOI: 10.35429/JQSA.2020.21.7.18.27 Received September 05, 2020; Accepted December 01, 2020

Abstract

One of the main disease caused by the COVID-19 in the humans is the pneumonia. This disease mainly attacks the lungs and one of the effective methods for diagnosis is through X-ray chest analysis. Due this in this work a methodology that allow the segmentation and analysis of regions that belong to the lungs in images of X-ray chest is presented. This methodology is based mainly in the implementation of some digital image processing techniques such as: contrast enhancement, segmentation, binarization and the application of morphological operations as the erosion and dilatation.

Viral pneumonia, bacterial pneumonia, image processing, analysis and segmentation of image

Resumen

Una de las principales afecciones ocasionadas por el COVID-19 en los seres humanos es la neumonía, enfermedad que ataca a los pulmones y uno de los métodos más eficaces para el diagnóstico certero de esta enfermedad es mediante el análisis de una radiografía torácica. Debido a esto en este trabajo se presenta una metodología que permite la segmentación y análisis de regiones que pertenecen a pulmones en imágenes de rayos X de torax. La metodología está basada principalmente en la implementación de algunas técnicas de procesamiento digital de imagen tales como: mejora del contraste, segmentación, binarización y la aplicación de operaciones de morfología matemática como la erosión y la dilación.

Neumonía viral, procesamiento de imagen, análisis y segementación de imagen

Citación: QUINTANILLA-DOMÍNGUEZ, Joel, YAÑEZ-VARGAS, Juan Israel, BUTANDA-SERRANO, Miriam and SÁNCHEZ-TORRECITAS, Enrique. Analysis and automatic segmentation of images for lungs regions extraction in X-ray chest. Journal of Quantitative and Statistical Analysis. 2020. 7-21: 18-27

* Correspondence to Author (email: jquintanilla_ptc@upjr.edu.mx)
† Investigador contribuyendo como primer autor.

Introduction

In recent months, millions of people around the world have contracted the coronavirus disease 2019 (COVID-19), which is caused by the SASR-COV-2. Currently, various investigations have shown that the most recurrent symptoms due to COVID-19 are fever, dry cough, fatigue and dyspnea. According to (Goërtz, et al., 2020) it shows that three months after COVID-19, more than 90% of the patients presented symptoms, with fatigue and dyspnea being the most reported. However, symptoms related to lung diseases were also reported as frequent, including Chronic Obstructive Pulmonary Disease (COPD) as well as Acute Hypoxemic Respiratory Failure (HARF) (Figueira Gonçalves, García-Talavera, Golpe, & Gurbani, 2020). These last two diseases, if not treated properly, can cause complications such as: heart problems, lung cancer, high blood pressure in pulmonary arteries and pneumonia, the latter being the subject of interest for the development of this work.

According to the World Health Organization, pneumonia is a type of acute respiratory infection that affects the lungs and is generally transmitted by direct contact with infected people (WHO, 2020). Pneumonia is classified mainly into typical or bacterial pneumonia and atypical pneumonia produced by viruses or atypical Bacterium (Echevarría, Miguel, Artigao, & del Castillo Martín, 2014). For the diagnosis of this disease, the doctor relies mainly on a physical examination specifically in the pulmonary region in order to detect any abnormal sound that suggests the presence of nemonia. If there is a suspicion of the disease, the doctor will request one of the following tests: blood chemistry, chest X-ray, pulse oximetry, sputum test and if the patient is over 65 years old, a chest CT image and culture of the chest may be included. pleural fluid (Mayo Clinic, 2020).

In (Polap & Wozniak, 2017) they present a lung segmentation technique based on graphic processing methods and a swarm algorithm. The swarm algorithm was used to extract particular regions of information and then use them in a detector based on a convolutional neural network.

In (Naranjo Alcázar, Bosch Roig, Sanz Requena, & Vázquez Martínez, 2016) present an automatic method of image analysis and segmentation for the detection of pulmonary nodules in chest radiographs. The segmentation of the lungs is mainly based on the application of the k-means clustering algorithm in addition to the application of mathematical morphology operations.

In (Joykutty, Satheeshkumar, & Samuvel, 2016) present a method for the automatic detection of tuberculosis using adaptive thresholding in chest radiography. The method consists of three stages. The first stage consists of segmentation of the region of the lungs using adaptive thresholding. The second stage consists of a feature extraction, finally in the third stage, a k-nn classifier is implemented to decide whether the image is normal or not. In this work, the second stage is of interest since this is where the region of the lungs is segmented, which is based on the implementation of image processing techniques such as contrast enhancement, binarization and the application of the morphology operation. math. It is important to highlight that part of this methodology was the one used in the present work for the segmentation of lung regions in chest radiographs.

This work focuses on the analysis of chest X-ray images in order to segment the lung region and thus help the doctor to improve the diagnosis of viral or bacterial pneumonia. For this, a methodology based mainly on image processing techniques such as contrast enhancement, segmentation, binarization and the application of mathematical morphology operations is implemented.

The work presented here is organized as follows: this section shows the introduction to the problem, as well as a brief state of the art on which the work is focused. Section 2 describes the development and implementation of the methodology. The results are shown in section 3. Finally, section 4 presents the conclusions of the work carried out.

ISSN 2410-3438

Proposed methodology

Database

The main requirement for image analysis is the database. In this work, the proposed methodology was applied to the database of chest radiography images known as Chest x-Ray Images Pneumonia. This database is classified into pneumonia and normal images. In turn, pneumonia images are classified as viral pneumonia and bacterial pneumonia images (Mooney, 2018). Figure 1 shows three chest x-ray images with a normal diagnosis, pneumonia due to Bacterium and pneumomy due to viruses, respectively.

(a) (b) (c)

Figure 1 Chest X-ray images extracted from the database. (a) Radiograph with normal diagnosis. (b) X-ray with diagnosis of bacterial pneumonia. (c) X-ray with virus diagnosis

Contrast enhancement

Image enhancement techniques are generally used to highlight one or some characteristics that are of interest in order to make their perception simpler for the human visual system (Quintanilla, Ojeda, Ruelas, & Yañez, 2019). Improvement techniques can be grouped into two categories, techniques in the spatial domain and techniques in the spatial domain. In this work, a technique is applied in the spatial domain since these are characterized by the direct manipulation of the image pixels (Gonzalez & Woods, 2002).

In the proposed methodology, the technique to be implemented as a contrast enhancement is the negative of the image. This is a pixel operation in which the value of the pixels of the regions that are light in dark and those that are dark in light is altered.

This image improvement can be very useful when you want to appreciate bright details in the image, that is, when there are bright regions in a dark background, for example in the case of chest X-rays, it is better to differentiate the region corresponding to the lung in order to find the lesions caused by pneumonia. The operation to make the negative of an image is defined as:

$$G = (L - 1) - I \quad (1)$$

Where G is the negative of the original image I and L is the highest level of gray intensity in the original image. Figure 2 shows the original images and images processed by applying the image negative.

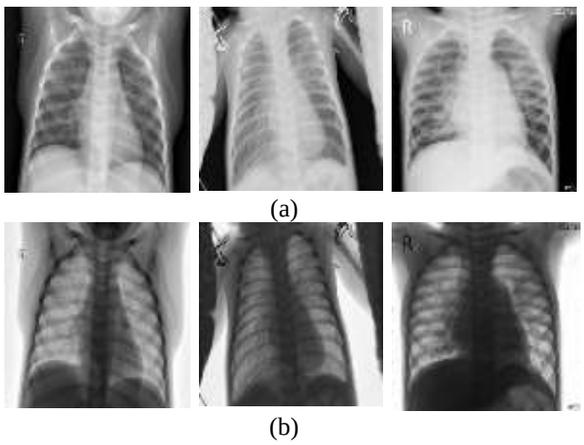

(a)

(b)

Figure 2 Contrast enhancement applying image negative. (a) Original chest radiograph images. (b) Chest X-ray images processed with the image negative

Segmentation

Segmentation is one of the most important stages of image processing and the purpose of this is to divide the image into small regions with respect to one or more characteristics such as: the level of gray intensity, color or texture. Gray level image segmentation techniques are generally based on one of the properties of gray level values such as discontinuity and similarity.

In this work, the objective of segmentation is to separate the X-ray image into different regions such as the fundus, lungs and bones, as well as tissue. To do this, a similarity-based technique known as multiple thresholding will be used using the Otsu method. Otsu's method of multiple thresholding or multi-thresholding allows to group the pixels of an image in several regions:

ISSN 2410-3438

$C_0 = \{1, \dots, u_1\}$,

$C_1 = \{u_1 + 1, \dots, u_2\}$, ...,

$C_n = \{u_n, \dots, L - 1\}$

Where L is the maximum value of gray levels of a pixel and where each class groups all the pixels up to a threshold obtained by Otsu, being:

$U = \{u_1, u_2, \dots, u_n\}$

the set of thresholds obtained. The way that Otsu's method selects the threshold value is by maximizing the variance between the regions, σ^2,

$$U = \underbrace{argmax}_{1 \le u_1 < u_2 \dots < u_n < L} \{\sigma^2\}$$

And the variance between the groups can be determined as:

$$\sigma^2 = \sum_{k=1}^{n} \omega_k \, (\mu_k - \mu_T)^2$$

Where:

$$\mu_k \sum_{i \in C_k} \frac{i * p_i}{\omega_k}$$

$$\omega_k = \sum_{i \in C_k} p_i \, , \omega_1 = \sum_{i=1} p_i, \dots, \omega_n = \sum_{i=u_{n+1}}^{L-1} p_i$$

$$\mu_T = \sum_{i \in C_k} \mu_k = \sum_{i=1}^{L-1} i * p_i$$

Where μk is the mean of the group or region Ck, μk is the probability that the pixels belong to class Ck, μT is the global mean of the image, and pi is the pixels with intensity of gray level i. (Merzban & Elbayoumi, 2019) (Gil, Torres, & Ortiz, 2004). As can be seen in Figure 3, the images are shown segmented by the multi-threshold Otsu method. To carry out this task, two threshold values were determined to segment the image into three regions. These values were obtained optimally by applying a simple Otsu thresholding.

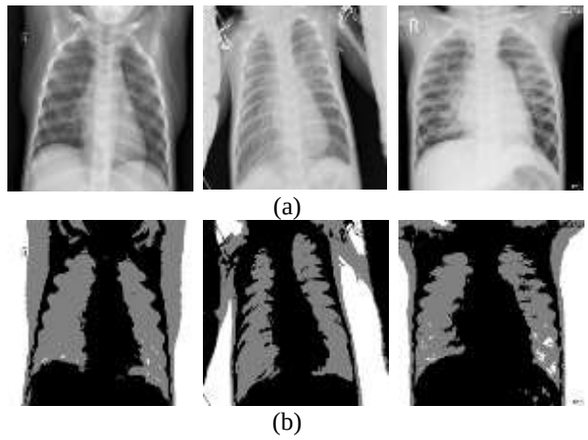

Figure 3 Image segmentation applying the multi-threshold Otsu method. (a) Original chest radiograph images. (b) Chest X-ray images segmented by multi-threshold Otsu

Binarization

Binarization is also an image segmentation, but in this case it divides it into only two regions by means of a threshold value (u), that is:

$$\begin{cases} Si\ I(i,j) \ge u\ the\ pixel\ value\ is\ 1 \\ Si\ I(i,j) < u\ the\ pixel\ value\ is\ 0 \end{cases}$$

where I (i, j) is defined as the intensity value of a pixel in the image. In this work, once the image is segmented into the fundus, lungs and bones, as well as the tissue, now the objective is to have an image where the region of the lungs and bones can be differentiated from the rest of the regions present in the image of the radiography. Figure 4 shows the binary images where the regions corresponding to lungs and bones are highlighted.

Figure 4 Segmented Image Binarization Process

The objective of this work is to segment the region of the lungs and in Figure 4 the region corresponding to the lungs can be seen, but other regions that are not of interest for analysis are still present. To solve the problem of eliminating regions that are not of interest, it is necessary to apply some other image processing techniques, including mathematical morphology operations, which will be presented in the next subsection.

ISSN 2410-3438

Mathematical morphology operations

Mathematical morphology operations are a very powerful tool in image analysis and processing since it is responsible for extracting, modifying and combining the components of an image that are useful in the representation and description of a region (Gonzalez & Woods, 2002). Currently there is a great diversity of applications related to image processing, in which segmentation, contrast enhancement and edge detection are involved. Initially, mathematical morphology operations were developed for binary images and later extended for images at gray levels. These operations allow the extraction of geometric structures from an image to transform or improve them according to some defined purpose, and for this a processing operator known as a structure element or structuring element (SE) is used. The SE is a fully defined assembly characterized by its shape and size and these depend on the purpose of the application. In addition, it has a point of reference known as the origin. In general, the SE is much smaller than the image with which it will interact. The two basic morphological operations are erosion and dilation.

The morphological erosion of an image corresponds to the minimum value of the function within an environment defined by the size and shape of the SE. Erosion is defined as:

$$I_{SE}^{E} = \min\{I(x+i, y+j) - SE(i,j)\}$$

The purpose of applying erosion to the binary image is in order to eliminate those regions that are smaller than the structuring element. In this work, the SE that he implemented to interact with the binary image is of the disk type with a radius of one pixel. Figure 5 shows the result of the application of erosion in the binary images.

Figure 5 Erosion process of the binarized image

Once those regions that are smaller than the SE have been eliminated, now the objective is to only leave the regions corresponding to the lungs and to carry out this task it is necessary to apply a technique that eliminates these regions. An unwanted region removal operation is used for this. This is one of the most used applications of morphological reconstruction (Gonzalez & Woods, 2002). Figure 6 shows the result of eliminating these regions.

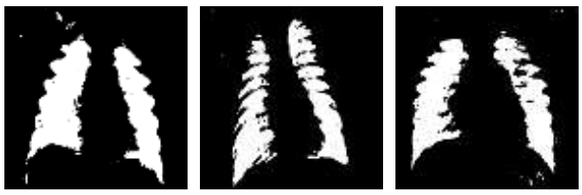

Figure 6 Segmentation of lung regions after removal of regions not of interest

In these images, only the regions corresponding to the lung can be seen. Likewise, it is possible to see groups of pixels that belonged to the regions that are not of interest and that were not eliminated in the previous processing. For this, it is necessary to apply operations such as dilation and morphological opening to conclude with the process of correct identification of the regions corresponding to the lung.

The morphological dilation of an image corresponds to the maximum value of the function within an environment defined by the size and shape of the SE. Dilation is defined as:

$$I_{SE}^{D} = \max\{I(x+i, y+j) - SE(i,j)\}$$

Figure 7 shows the resulting images after applying the dilation process. In these images it can be seen that the gaps that were present have been filled as a product of morphological dilation. Likewise, it can be seen that there are some regions that do not belong to the regions of the lungs and it is necessary to remove them for this, the morphological opening operation is applied.

Figure 7 Images resulting from the process of morphological dilation

The combination of erosion and dilation operations is the basis for creating other operations which are also used for image processing applications. The morphological opening of an image is defined as erosion followed by dilation using the same SE. This operation is expressed as:

$$I \circ SE = (I \ominus SE) \oplus SE$$

Where $\ominus$ denotes the erosion operation and $\oplus$ the dilation operation, respectively. The morphological aperture is generally responsible for removing small and clear objects relative to the size of the SE. On the other hand, it maintains the size of large and bright objects. This is due to the fact that the erosion is carried out first and this is in charge of eliminating the small details at the same time that the image darkens and later the dilation is in charge of increasing the brightness, but without introducing the objects eliminated by the erosion (Gonzalez & Woods, 2002).

Figure 8 Resulting images after applying the morphological opening process

In Figure 8 you can see the result of the morphological opening where the regions that do not belong to the lungs have been eliminated. On the other hand, it can also be seen that in the regions that correspond to the lung there are some small empty regions. To solve this problem, a region filling technique has been applied and the result can be seen in Figure 9.

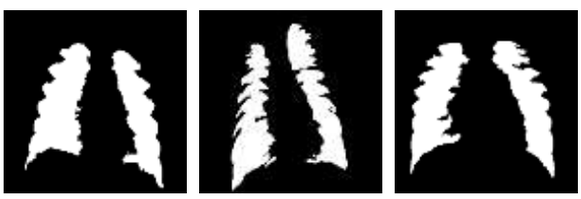

Figure 9 Images resulting from the region fill process

In Figure 9 you can see the regions corresponding to the lung already segmented from the original images. Figure 10 (a) shows the original chest X-ray images. Figure 10 (b) shows only the segmented regions corresponding to lungs obtained with the proposed methodology and highlighted on a black background. Finally, Figure 10 (c) shows the original images with the outline highlighted in red corresponding to the lung regions found with the methodology proposed in this work.

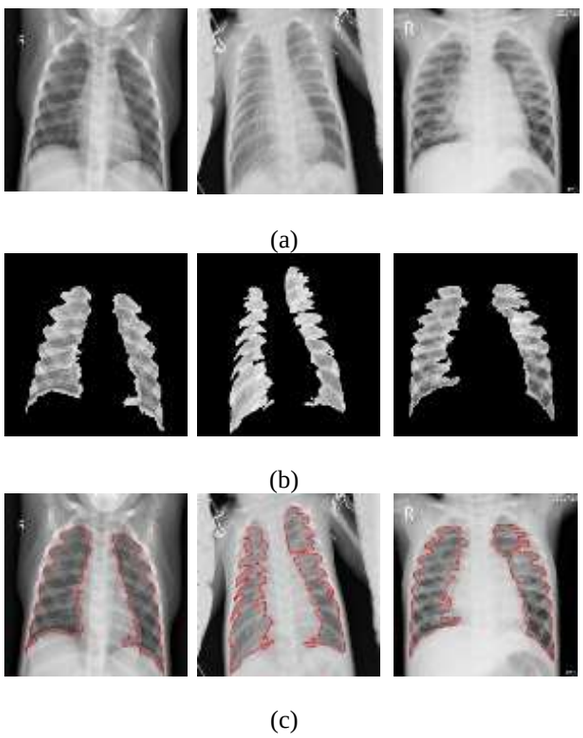

(a)

(b)

(c)

Figure 10 Result of the segmentation process of the regions corresponding to the lung in chest X-ray through the proposed methodology. (a) Original chest X-ray images. (b) Segmented regions corresponding to lungs obtained with the proposed methodology and highlighted on a black background. (c) Original images with the outline highlighted in red corresponding to the lung regions found with the proposed methodology

Results

Table 1 shows the analysis of an experiment that was performed with 30 chest X-ray images from the database used for this work. 10 of the images correspond to a normal diagnosis, 10 to bacterial pneumonia and 10 to virus pneumonia.

ISSN 2410-3438

Image	Diagnosis	Segmentation of both lungs		Observations
		Yes	No	
1	Normal	✓		
2	Normal	✓		
3	Normal	✓		
4	Normal	✓		
5	Normal	✓		
6	Normal		✓	Segment the left lung
7	Normal	✓		
8	Normal	✓		
9	Normal	✓		
10	Normal	✓		
11	Bacterium		✓	Segment the left lung and a couple of regions of the right
12	Bacterium		✓	Does not segment either of the two lungs
13	Bacterium	✓		
14	Bacterium	✓		
15	Bacterium		✓	Does not segment either of the two lungs
16	Bacterium		✓	Segment the left lung and a couple of regions of the right
17	Bacterium		✓	Does not segment either of the two lungs
18	Bacterium		✓	Segment the left lung and a couple of regions of the right
19	Bacterium		✓	Segment only a couple of regions of the right
20	Bacterium		✓	Does not segment either of the two lungs
21	Virus	✓		
22	Virus	✓		
23	Virus		✓	Segment the left lung and a couple of regions of the right
24	Virus		✓	Does not segment either of the two lungs
25	Virus	✓		
26	Virus	✓		
27	Virus		✓	Segment the left lung and a couple of regions of the right
28	Virus	✓		
29	Virus		✓	Segment the left lung
30	Virus		✓	Segment the right lung

Table 1 Analysis of the results obtained applying the proposed methodology

As can be seen in Table 1, in 16 radiographs the proposed methodology was able to segment the regions corresponding to the lung, of which 9 are with a normal diagnosis, 2 with a diagnosis of bacterial pneumonia and 5 with a diagnosis of viral pneumonia, see Figure 11.

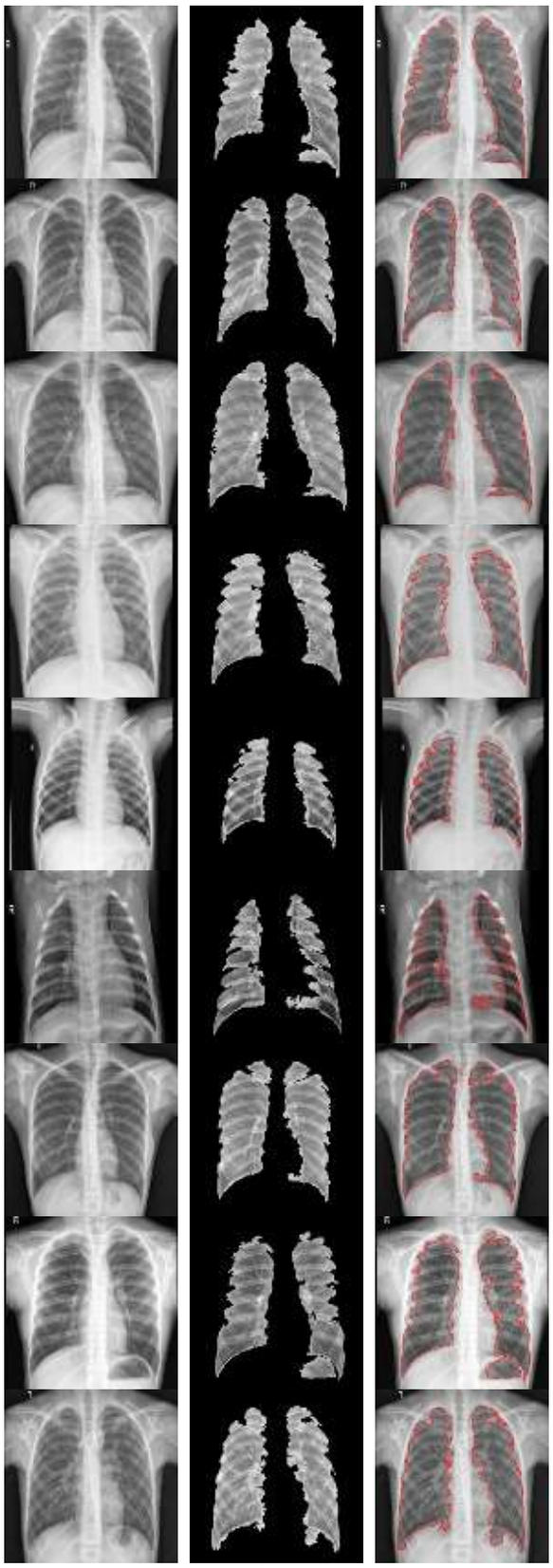

(a)

ISSN 2410-3438

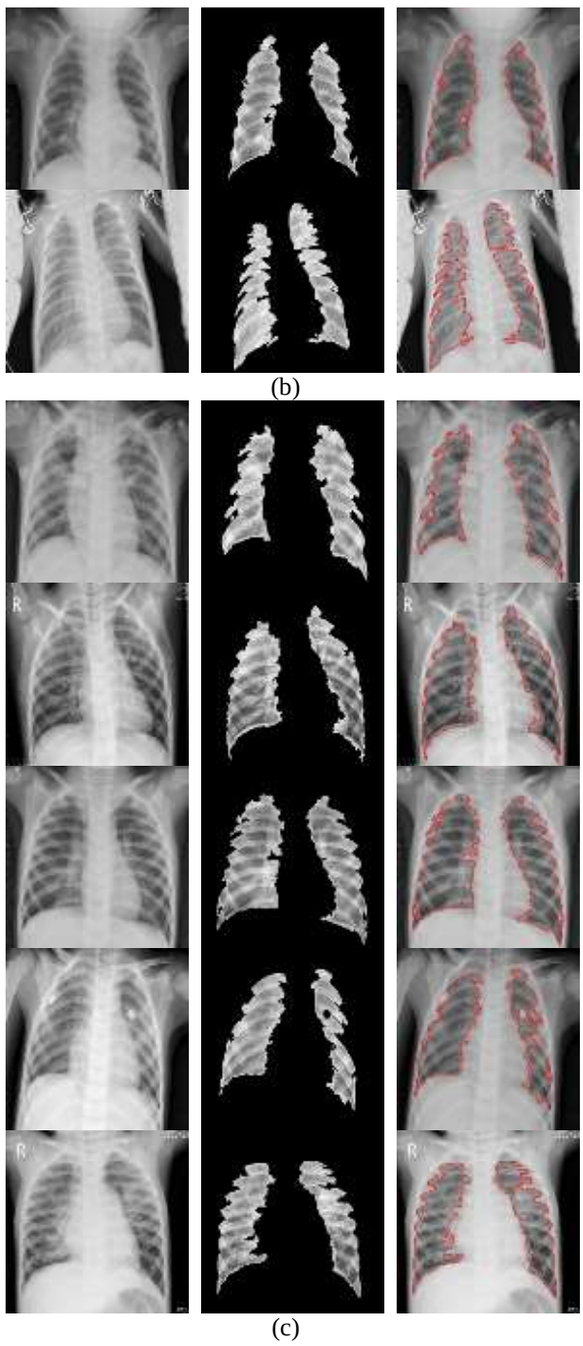

Figure 11 Results of the segmentation of the radiography images applying the proposed methodology detecting both regions corresponding to the lung. (a) Segmentation of lungs with normal diagnosis. (b) Segmentation of lungs with diagnosis of bacterial pneumonia. (c) Segmentation of lungs with diagnosis of viral pneumonia.

Of the 14 X-rays that the methodology could not segment the two regions corresponding to the lungs in 3 X-ray images, it segments only one of the lungs, of which one has a normal diagnosis and 2 with a diagnosis of viral pneumonia as shown in Figure 12.

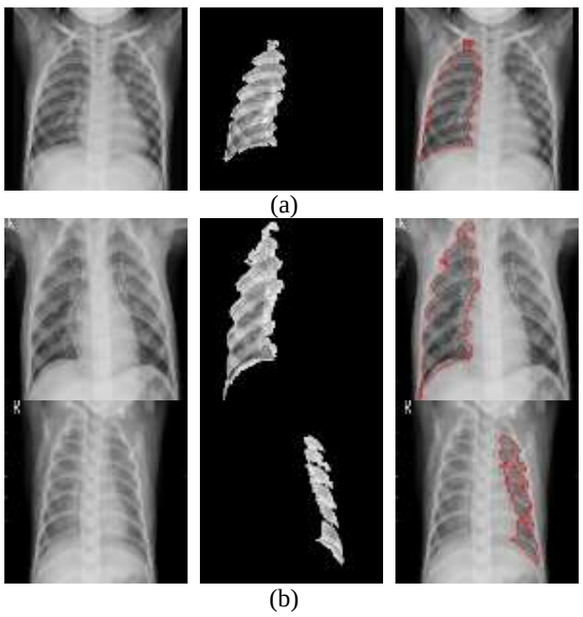

Figure 12 Results of the segmentation of the radiography images applying the proposed methodology detecting only one region corresponding to the lung. (a) Segmentation of a lung with normal diagnosis. (b) Segmentation of a lung diagnosed with viral pneumonia.

In 6 radiographs, he segmented one of the lungs and some regions of the other, of which 4 have a diagnosis of bacterial pneumonia and 2 with a diagnosis of viral pneumonia as shown in Figure 13.

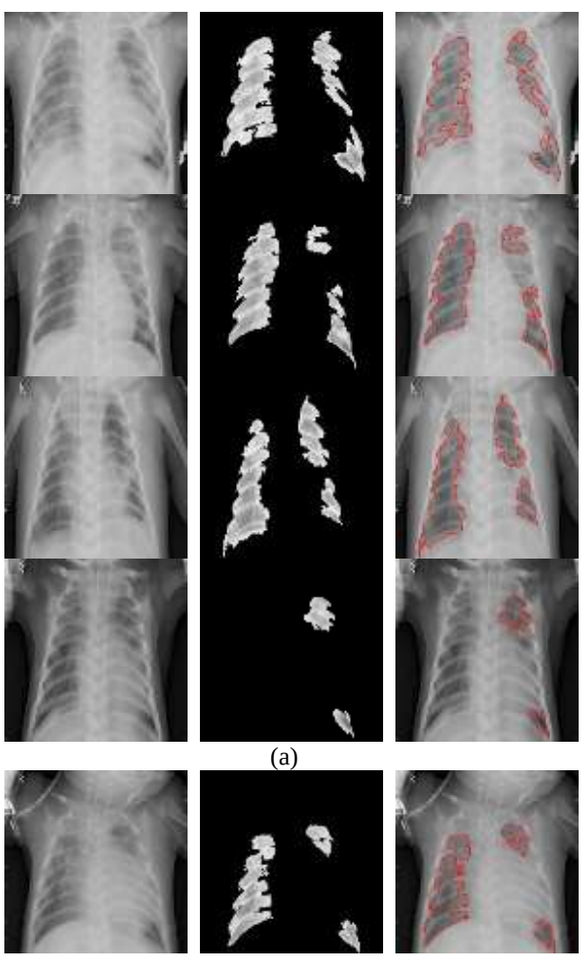

(b)

Figure 13 Results of the segmentation of the X-ray images applying the proposed methodology, detecting only one region corresponding to the lung and some regions of the other lung. (a) Radiographs with a diagnosis of bacterial pneumonia. (b) X-rays with diagnosis of viral pneumonia

Finally, in 5 of the radiographs the methodology does not segment either of the two lungs, of which 3 are diagnosed with bacterial pneumonia and 2 with viral pneumonia.

According to the results obtained by applying the proposed methodology, it can be seen that in 83.3% of the radiography images used for this work, the regions corresponding to the lung were segmented in a satisfactory way. While 16.6% failed to detect any of the regions corresponding to the lung.

Conclusions

In this work, a methodology based on digital image processing techniques for the segmentation of chest radiography images was presented to segment the regions corresponding to the lung. The methodology presented is mainly composed of contrast enhancement, segmentation, binarization, and mathematical morphology operations. According to the results obtained, it is appreciated that the methodology can segment the lung regions with a good percentage. It is evident that the methodology did not manage to segregate all the images as expected, it has areas of opportunity that can be improved by applying some other image processing techniques. On the other hand, it is necessary to have segmented images of the regions corresponding to the lung by experts in order to be able to measure the accuracy of the segmentation of the proposed methodology. Likewise, as future work, an analysis of the regions corresponding to the lung can be proposed through the application of another methodology applying some other image segmentation technique so that the type of lesion found in the region of interest is automatically determined.

Finally, it is concluded that the proposed methodology can be used as an image analysis tool that can be of great help as a complement for the diagnosis of bacterial or viral neumnia due to the disease that is currently causing millions of deaths in the world population. as is COVID-19.

Acknowledgments

The authors refer to the National Council for Science and Technology (CONACyT), the Department of Engineering in Networks and Telecommunications and the Master's Degree in Engineering (Intelligent Systems) of the Polytechnic University of Juventino Rosas (UPJR) and Dr. César Centeno Fosado and the Nurse Liliana Yañez Vargas of the Salmanca State Center for Critical Care for supporting this work.

References

Echevarría, A., Miguel , M., Artigao, F., & del Castillo Martín, F. (2014). Neumonía adquirida en la comunidad. *Protocolos diagnósticos terapéuticos de la AEP: Infectología pediátrica.*, 59-66.

Figueira Gonçalves, J., García-Talavera, I., Golpe, R., & Gurbani, N. (2020). Síndrome post-COVID en el paciente con enfermedad pulmonar obstructiva crónica: ¿Un caballo de Troya? *Medicina de Familia. SEMERGEN*, 1-2. doi:https://doi.org/10.1016/j.semerg.2020.10.002

Gil, P., Torres, P., & Ortiz, F. (2004). Detección de Objetos por Segmentación Multinivel Combinada de Espacios de Color. 1-7.

Goërtz, Y., Van Herck, M., Delbressine, J., Vaes, A., Meys, R., Machado, F., & et al. (2020). Persistent symptoms 3 months after a SARS-CoV-2 infection: the post-COVID-19 syndrome? *ERJ open research*, 1-20.

Gonzalez, R., & Woods, R. (2002). *Digital Image Processing.* Prentice-Hall.

Joykutty, B., Satheeshkumar, K., & Samuvel, B. (2016). Automatic Tuberculosis Detection using Adaptive Thresholding in Chest Radiographs. *2016 International Conference on Emerging Technological Trends (ICETT)*, (págs. 1-7).

Mayo Clinic. (21 de Diciembre de 2020). *Mayo Clinic*. Obtenido de https://www.mayoclinic.org/es-es/diseases-conditions/pneumonia/diagnosis-treatment/drc-20354210

Merzban, M., & Elbayoumi, M. (2019). Efficient solution of Otsu multilevel image thresholding: A comparative study. *Expert Systems with Applications*, 299-309.

Mooney, P. (24 de Marzo de 2018). *Chest X-Ray Images (Pneumonia)*. Obtenido de https://www.kaggle.com/paultimothymooney/chest-xray-pneumonia

Naranjo Alcázar, J., Bosch Roig, I., Sanz Requena, R., & Vázquez Martínez, S. (2016). Método automático de análisis y segmentación de imágenes para la detección de nódulos pulmonares a partir de radiografías de tórax. *XXXIV Congreso Anual de la Sociedad Española de Ingeniería Biomédica*, (págs. 459-462). Valencia.

OMS. (21 de Diciembre de 2020). *Organización Mundial de la Salud*. Obtenido de https://www.who.int/topics/pneumococcal_infections/es/

Polap, D., & Wozniak, M. (2017). Lung segmentation on x-ray images with neural validation. *Połap, D., & Woźniak, M. (2017). Lung segmentation on x-ray images with neural validation. In 2017 IEEE Symposium Series on Computational Intelligence (SSCI)*, (págs. 1-7).

Quintanilla, J., Ojeda, B., Ruelas , R., & Yañez, J. (2019). Contrast enhancement of mammographic images by digital images processing. *Journal of Scientific and Technical Applications*, 19-28.

ISSN 2410-3438

Article **Journal of Quantitative and Statistical Analysis**
December, 2020 Vol.7 No.21 28-33

Relationship between electrostatic powder coating thickness measurements at different points on uneven surfaces

Relación entre medidas de espesor de recubrimento electrostático en polvo en diferentes puntos sobre superificies irregulars

LUÉVANO-CABRALES, Olga Lidia*†, SALAS-PÉREZ, Francisco Guillermo, JUÁREZ-DEL TORO, Raymundo and MORALES-VILLA, Julio César

ID 1st Author: *Olga Lidia, Luévano-Cabrales*

ID 1st Coauthor: *Francisco Guillermo, Salas-Pérez*

ID 2nd Coauthor: *Raymundo, Juárez-Del Toro*

ID 3rd Coauthor: *Julio César, Morales-Villa*

DOI: 10.35429/JQSA.2020.21.7.28.33 Received September 05, 2020; Accepted December 30, 2020

Abstract

Measure relation of electrostatic powder coating thickness at diferent points on irregular surfaces. In this work, we found the relation between the thickness measures at diferent areas of a irregular surface, by the electrostatic powder coating on pieces with five diferent geometries and varyin slightly parameters like potential and application distance. At the products where the electrostatic powder coating are used, the thickness measure is an importante quality characteristic, however on the irregular surfaces is so noticeable when the thickness measure is not uniform on the entire piece. But when it is known that the thickness ratio varies from one area to another of the same piece, it is easier to establish a methodology that allows the process to have a measure of uniform thickness.

Electrostatic Powder Coating, Thickness, Finite Element

Resumen

Relación entre medidas de espesor de recubrimento electrostático en polvo en diferentes puntos sobre superificies irregulares. En este trabajo se encuentra la relación entre las medidas de espesor de diferentes áreas de una superificie irregular, mediante la aplicación de recubrimiento electrostático en piezas con cinco geometrías diferentes y modificando levemente parámetros como potencial y distancia de aplicación. En los productos donde se utiliza el recubrimiento electrostático el espesor es una característica de calidad importante, sin embargo en las superficies irregulares es mas notorio cuando la medida de espesor no es uniforme en toda la pieza. Sin embargo cuando se conoce en que proporción varía el espesor entre un área y otra de la misma pieza, es mas fácil establecer una metodología en el proceso que permita tener una medida de espesor uniforme.

Recubrimiento electrostático en polvo, Espesor, Elemento finito

Citación: LUÉVANO-CABRALES, Olga Lidia, SALAS-PÉREZ, Francisco Guillermo, JUÁREZ-DEL TORO, Raymundo and MORALES-VILLA, Julio César. Relationship between electrostatic powder coating thickness measurements at different points on uneven surfaces. Journal of Quantitative and Statistical Analysis. 2020. 7-21: 28-33

* Correspondence to Author (email: oluevano@upgop.edu.mx)
† Investigador contribuyendo como primer autor.

Introduction

The application of electrostatic powder coating has been used since the 70's last century, and since its inception it was detected that it is complex to obtain a uniform thickness measurement in the coating layer, and when the substrate has a geometry irregular, that is, it was subjected to plastic deformation before the coating process, then it becomes more complex, since the deep regions in an irregular geometry cause the effect called the Faraday cage (EJF), which does not allow the dust particles reach the depths of the geometry.

In an electrostatic system for the application of electrostatic powder coating (for the case of this study it is paint), the electric field lines are directed from the electrode in the gun towards the substrate or surface to be covered, when the surface it is irregular so the electric field lines cancel out when reaching the deep regions so they do not penetrate to the bottom. The dust particles follow the electric field lines and since they do not penetrate to the deep regions then the dust does not reach either, causing smaller paint thickness measurements in those regions.

The effect of the Faraday cage in the electrostatic painting process has been known since this type of process arose; Efforts to solve it focus on controlling some individual or group parameters such as current intensity (Guskov, 1996), the amount of charge with respect to the mass of the dust cloud Q / m (Biris, 2011), the size of the particle (Rupp, 2012), etc.

Some equipment for the application of electrostatic powder paint, such as the WAGNER, have integrated programs with combinations of parameters appropriate to the type of surface to be covered; These surfaces are classified as flat surfaces, large surfaces and irregular surfaces, however the problem is not solved in a definitive way, and it is complicated because the EJF is inherent to electric fields on irregular surfaces, which means that it is not possible to eliminate it. completely, so research is focused on mitigating it in some way.

Since the uniformity of the thickness measurement over the entire surface is an important characteristic to evaluate the quality of the product, it is considered advisable to carry out a study in which it is identified how the thickness measurement varies throughout the surface, and is related to the electric field intensity.

With this objective, an experiment was designed with five types of surface which were covered by the electrostatic powder coating process to later measure the thickness at eight different points of each type of surface and thus determine the spatial variation in the measurement of thickness of each surface.

The structure of this document contemplates first the description of the electrostatic system, then a brief explanation of the finite element method, the materials, equipment and experimentation are specified, the results obtained and the general conclusions.

Electrostatic system

The set of equipment and materials that is needed to apply electrostatic coating either in powder or liquid is called electrostatic system, this study focuses on powder painting as electrostatic coating and in this section it is explained how is the paint application process and how to simulate electrostatic fields using the finite element method.

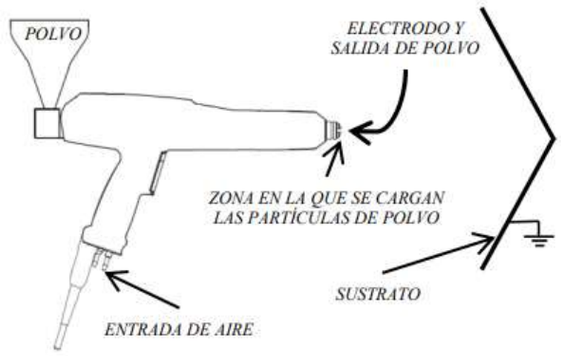

Figure 1 Electrostatic gun and substrate (drawing obtained from supplier's manual)

Equipment for electrostatic process

An electrostatic system for the coating process (Figure 1), includes an electrostatic gun with an electrode connected to a high voltage generator and a substrate connected to ground.

The gun is connected to a compressor, the air from the compressor drives the dust particles around the electrode, where the discharge corona is formed and the particles are negatively charged and with the force of the electric field are directed towards the substrate.

ISSN 2410-3438

When the download is generated in the When the download is generated in the gun, an electric field is formed between the gun and the substrate. The electric field intensity is known by the potential gradient, which is represented as u *(x, y):*

$$\mathbf{E} = -\nabla u(x,y) \tag{1}$$

La relación entre el campo eléctrico y la densidad de carga ρ está dada por:

$$\varepsilon \nabla \cdot \boldsymbol{E} = \rho \tag{2}$$

Where ε is the permittivity of the material, substituting equation (1) in equation (2); the result is the Poisson equation of potential:

$$\Delta u(x,y) = -\frac{\rho}{\varepsilon} \tag{3}$$

The Poisson equation (3) describes how the potential and electric field lines are distributed. To solve this equation in an electrostatic system it is feasible to use the finite element method.

The finite element method in electrostatics

The finite element method has different ways of solving partial differential equations, one of the most used is the variational method. This method uses a functional, which is an expression of the potential energy in the domain. Through the minimization of the energy in each element, the electric field lines are obtained in the entire region. The equation to be solved for the electric field is the Poisson equation. Limit constraints are Dirichlet and / or Neumann conditions. The functional of the equation is:

$$I = \int_A \left\{ \frac{1}{2}\varepsilon_0 \left(\frac{\partial \Phi}{\partial x}\right)^2 + \frac{1}{2}\varepsilon_0 \left(\frac{\partial \Phi}{\partial y}\right)^2 \right\} dA - \oint \Phi \frac{\partial \Phi}{\partial n} dR \tag{4}$$

Where A corresponds to the region of integration, Φ is the potential and I is the functional. The first part of the functional represents the energy of the electric field.

By means of discretization, each element is defined according to a function, the number of its nodes and the potential, which is defined by the potential at the nodes.

$$\Phi = |N|(\Phi)^e = (N_i, N_j, N_k) \begin{vmatrix} \Phi_i \\ \Phi_j \\ \Phi_k \end{vmatrix} \tag{5}$$

Where | N | is the matrix of functions of form. To find the minimum energy potential, the functional must be partially derived with respect to each node. Therefore:

$$\frac{\partial I^e}{\partial \Phi^e} = |K|^e \{\Phi\}^e \tag{6}$$

The matrix of each element is assembled into a global matrix and boundary conditions are applied.

$$|\mathbf{K}|\{\mathbf{U}\} = \{\mathbf{P}\} \tag{7}$$

K represents the stiffness matrix, U is the vector of unknown potentials and P is the solution vector.

Methods

The experimentation was conducted in two ways, the first to calculate the field electrical using the finite element method and the second to measure the thickness of the paint cured on the treated surface.

Design of experiments

An experiment was designed with 5 different geometries, three with angles of 60 °, 90 ° and 120 ° and two with a box shape with 1 ”depth and the width of the deep region in the first 1” and in the second of 2 ”(Figure 2), the material is low carbon steel, the paint used was Krhal, the variables to be measured are paint thickness in mils and electric field intensity in V / m.

Two different types of parameter combinations were used, each combination will be called treatment from here from now on, the first type of treatment is oriented towards measuring the thickness of paint and is numbered from one to eight (Table 1), the second type of treatment is for the calculation of the electric field intensity, said calculation was made the finite element method and the treatments are identified with the letters A, B, C and D (Table 2).

ISSN 2410-3438

A 200 ° C convection oven was used to cure the paint for 10 minutes and a Positector 6000 thickness gauge was used.

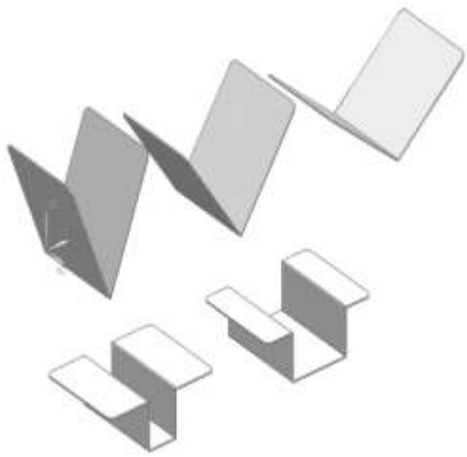

Figure 2 Five different geometries

Tratamientos Para Espesor			
Tratamiento	Voltaje (kV)	Distancia (cm)	% Polvo
1	70	15	50
2	70	15	60
3	60	15	50
4	60	15	60
5	70	20	50
6	70	20	60
7	60	20	50
8	60	20	60

Table 1 Parameters for measuring coating thickness

Electric Field Intensity		
Tratamiento	Voltaje (kV)	Distancia (cm)
A	70	15
B	60	15
C	70	20
D	60	20

Table 2 Parameters for calculating electric field

Electric field strength calculated with the finite element method

To calculate the electric field intensity, COMSOL® was used, a three-dimensional domain was established, forming a block in the shape of a rectangle, the small faces of the rectangle are found in the upper and lower part of the block, in the center of the upper face a point is located that represents the electrode, and the lower face takes the shape of the geometry to be analyzed (Figure 3); the boundary conditions were Dirichlet for the electrode with u = V and for the grounded substrate with u = 0, the rest of the boundaries are Neumann with $\partial u(x, y, z) / \partial x = \partial u(x, y, z) / \partial y = \partial u(x, y, z) / \partial z = 0$.

The calculation was made in eight different points of each piece (Figure 4), the same ones where the measurements of the thickness of the paint were made.

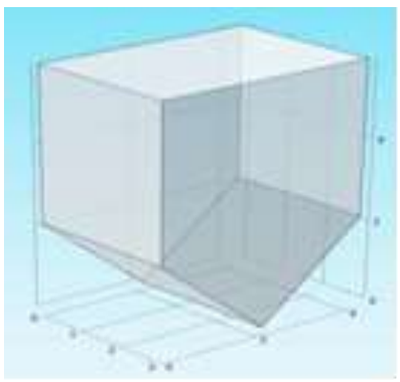

Figure 3 Domain

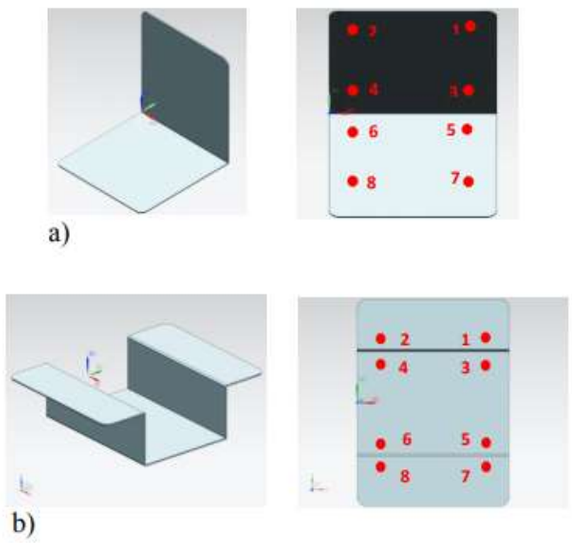

Figure 4 a) Points where thickness was measured in geometries with a center bend, b) Points where thickness was measured in geometries with deep regions

Results

The electric field intensity values were obtained at each point indicated, in the same way the thickness was measured at the same points and when graphing the results, similar patterns of variation were found between the electric field intensity graphs and those of the thickness, the Table 3 shows graphs of two of the geometries.

ISSN 2410-3438

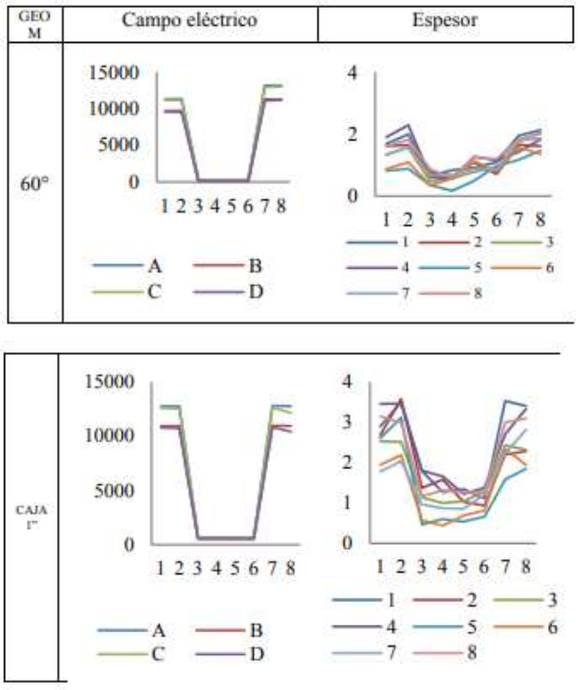

Table 3 Graph of electric field intensity and thickness of two different geometries

When it was observed that the behavior of the variation of the electric field intensity resembles the behavior of the variation of the thickness, the relationship between both parameters was measured by means of a correlation coefficient and it was found that the smallest correlation value is 67 % (table 4) which indicates that the thickness measurement is explained through the behavior of the electric field intensity at each measurement point.

Geom	A - 1	A -2	B - 3	B - 4	C - 5	C - 6	D - 7	D - 8
60°	0.9659	0.9510	0.9415	0.8031	0.7659	0.7266	0.9591	0.9053
90°	0.8689	0.7107	0.8801	0.8865	0.7759	0.7650	0.7948	0.7250
120°	0.7217	0.8823	0.7177	0.7389	0.7010	0.6906	0.6720	0.7868
1"	0.9606	0.8622	0.9896	0.9011	0.8959	0.9809	0.8996	0.9973
2"	0.9747	0.9636	0.9741	0.8982	0.9852	0.9874	0.9779	0.9474

Table 4 Treatment correlation

Discussion

The thickness measurements on an irregular surface have important differences when comparing the thicknesses of the deep regions with the thicknesses of the upper regions, this is When the parameters that affect the thickness measurement are analyzed, the electric field intensity is not considered, however when reviewing the behavior of the thickness measurement in the eight measurement points and it was related to the measurement of the intensity and Electric field at the same points is observed as having similar variation patterns and when calculating the correlation between both parameters.

It was found that the smallest correlation value is 67% and the largest is 99%, in addition the 50th percentile is 89% , which indicates that the smallest correlation values are more dispersed than the highest values. With the information obtained, it can be seen that the electric field intensity is a parameter that deserves to be more important if you want to control the uniformity of the thickness on an irregular surface due to the effect of the Faraday cage.

References

Casaux, J., (2007), Critical thickness of electrostatic powder coatings from inside, *Journal of electrostatic*, 2007; 65: 764 – 774.

Chen, Y., Liang, X., Bai, & J., Xu, B., (2010), Finite element modeling of coating formation and transient heat transfer in the electric arc spray process, *International Journal of heat and mass transfer*, 2012; 13, 2012 – 2021.

Guskov, S., (1996), Electrostatic phenomena in powder coating, *Powder coating '96,* Nordson Corporation, Indianapolis Indiana.

Hayt, W.H. Jr. & Buck, J.A., (2006), *Teoría electromagnética*, México, Mc Graw Hill Interamericana Editores S.A. de C.V., 7ª ed.

Humphires, S. Jr., (2010), *Finite element methods for electromagnetics,* electronic edition of "Field solution on computers", Ed. CRC Press a division of Taylor and Francis.

Hyuncheol, O., Kyoungtae, K., & Sangsoo, K., (2008), Characterization of deposition patterns produced by twin – nozzle electrospray, *Journal of aerosol science*, 2008; 39: 801–813.

Inculet, I.I., & Adamiak, K., (1993), Charge limits in corona charging of distorted liquid droplets, *IEEE Transactions on industry applications*, 1993; 29: 1058 – 1061.

Jalaal, M., Soleimani, S., Domairry, G., Ghasemi, E., Bararnia, H., Mohammadi, F. & Barari, A., (2011), Numerical simulation of electric field in complex geometries for different electrode arrangements using meshless local MQ-DQ method, *Journal of Electrostatic*, 2011; 69: 168 – 175.

ISSN 2410-3438

Kreeger, K., (1994), Application variables for powder coating systems, *Nordson Corporation*.

Lackowski, M., Krupa, A. & Jaworek, A., (2010), Corona discharge ion sources for fine particle charging, *The European Physical Journal D*, 2010; 377 – 382.

Le Moyne, L., (2010), Trends in atomization theory, *International journal of spray and combustion dynamics*, 2010; 1: 49 – 84.

Matsusaka, S. & Masuda, H., (2002), Theorical analysis of electrostatic forces between coated particles, *Advanced powder technology*, 2002; 13: 2: 157 – 166.

Nordson Corporation, (2004), Corona charging and electrostatics for pipe coating.

Plonus, M.A., (1994), *Electromagnetismo aplicado*, Barcelona, Editorial Reverté S.A.

Sarrate, J. & Clarisó, R., (2001), El método de los elementos finitos en problemas electromagnéticos: planteamiento y aplicaciones, *Revista internacional de métodos numéricos para cálculo y diseño en ingeniería*, 2001; 17: 1: 219 – 248.

Wu, Y., Castle, P. & Inculet, I.I., (2005), Induction charging of granular materials in an electric field, *IEEE Transactions on Industry Applications*, 2005; 41:1350 – 1357.

Ye, Q., Steigleder, T., Scheibe, A. & Domnick, J., (2002), Numerical simulation of the electrostatic powder coating process with a corona spray gun, *Journal of electrostatic*, 2002; 54: 189 – 205.

ISSN 2410-3438

Title in Times New Roman and Bold No. 14 in English and Spanish]

Surname (IN UPPERCASE), Name 1st Author†*, Surname (IN UPPERCASE), Name 1st Coauthor, Surname (IN UPPERCASE), Name 2nd Coauthor and Surname (IN UPPERCASE), Name 3rd Coauthor

Institutional Affiliation of Author including Dependency (No.10 Times New Roman and Italic)

International Identification of Science - Technology and Innovation

ID 1st Author: (ORC ID - Researcher ID Thomson, arXiv Author ID - PubMed Author ID - Open ID) and CVU 1st author: (Scholar-PNPC or SNI-CONACYT) (No.10 Times New Roman)

ID 1st Coauthor: (ORC ID - Researcher ID Thomson, arXiv Author ID - PubMed Author ID - Open ID) and CVU 1st coauthor: (Scholar or SNI) (No.10 Times New Roman)

ID 2nd Coauthor: (ORC ID - Researcher ID Thomson, arXiv Author ID - PubMed Author ID - Open ID) and CVU 2nd coauthor: (Scholar or SNI) (No.10 Times New Roman)

ID 3rd Coauthor: (ORC ID - Researcher ID Thomson, arXiv Author ID - PubMed Author ID - Open ID) and CVU 3rd coauthor: (Scholar or SNI) (No.10 Times New Roman)

(Report Submission Date: Month, Day, and Year); Accepted (Insert date of Acceptance: Use Only ECORFAN)

Abstract (In English, 150-200 words)

Objectives
Methodology
Contribution

Abstract (In Spanish, 150-200 words)

Objectives
Methodology
Contribution

Keywords (In English)

Indicate 3 keywords in Times New Roman and Bold No. 10

Keywords (In Spanish)

Indicate 3 keywords in Times New Roman and Bold No. 10

Citation: Surname (IN UPPERCASE), Name 1st Author, Surname (IN UPPERCASE), Name 1st Coauthor, Surname (IN UPPERCASE), Name 2nd Coauthor and Surname (IN UPPERCASE), Name 3rd Coauthor. Paper Title. Journal of Quantitative and Statistical Analysis. Year 1-1: 1-11 [Times New Roman No.10]

* Correspondence to Author (example@example.org)
† Researcher contributing as first author.

Introduction

Text in Times New Roman No.12, single space.

General explanation of the subject and explain why it is important.

What is your added value with respect to other techniques?

Clearly focus each of its features

Clearly explain the problem to be solved and the central hypothesis.

Explanation of sections Article.

Development of headings and subheadings of the article with subsequent numbers

[Title No.12 in Times New Roman, single spaced and bold]

Products in development No.12 Times New Roman, single spaced.

Including graphs, figures and tables-Editable

In the article content any graphic, table and figure should be editable formats that can change size, type and number of letter, for the purposes of edition, these must be high quality, not pixelated and should be noticeable even reducing image scale.

[Indicating the title at the bottom with No.10 and Times New Roman Bold]

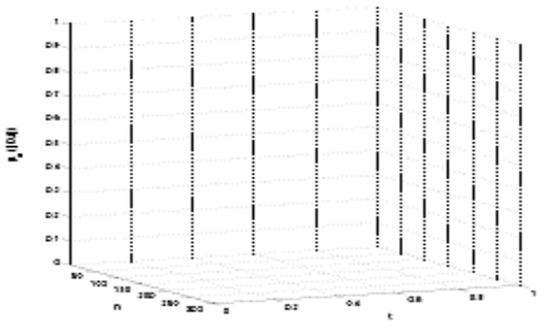

Graphic 1 Title and *Source (in italics)*

Should not be images-everything must be editable.

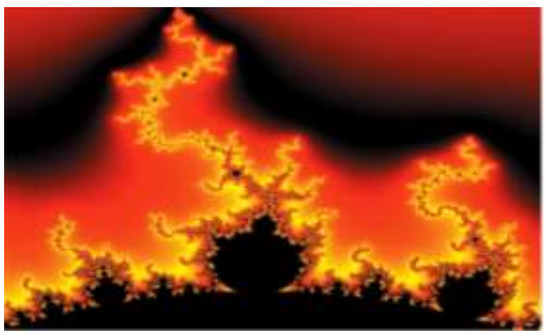

Figure 1 Title and *Source (in italics)*

Should not be images-everything must be editable.

Table 1 Title and *Source (in italics)*

Should not be images-everything must be editable.

Each article shall present separately in **3 folders**: a) Figures, b) Charts and c) Tables in .JPG format, indicating the number and sequential Bold Title.

For the use of equations, noted as follows:

$$Y_{ij} = \alpha + \sum_{h=1}^{r} \beta_h X_{hij} + u_j + e_{ij} \qquad (1)$$

Must be editable and number aligned on the right side.

Methodology

Develop give the meaning of the variables in linear writing and important is the comparison of the used criteria.

Results

The results shall be by section of the article.

Annexes

Tables and adequate sources

Thanks

Indicate if they were financed by any institution, University or company.

Conclusions

Explain clearly the results and possibilities of improvement.

ISSN 2410-3438

References

Use APA system. Should not be numbered, nor with bullets, however if necessary numbering will be because reference or mention is made somewhere in the Article.

Use Roman Alphabet, all references you have used must be in the Roman Alphabet, even if you have quoted an Article, book in any of the official languages of the United Nations (English, French, German, Chinese, Russian, Portuguese, Italian, Spanish, Arabic), you must write the reference in Roman script and not in any of the official languages.

Technical Specifications

Each article must submit your dates into a Word document (.docx):

Journal Name
Article title
Abstract
Keywords
Article sections, for example:

1. Introduction
2. Description of the method
3. Analysis from the regression demand curve
4. Results
5. Thanks
6. Conclusions
7. References

Author Name (s)
Email Correspondence to Author
References

Intellectual Property Requirements for editing:

-Authentic Signature in Color of Originality Format Author and Coauthors

-Authentic Signature in Color of the Acceptance Format of Author and Coauthors

ISSN 2410-3438

Reservation to Editorial Policy

Journal of Quantitative and Statistical Analysis reserves the right to make editorial changes required to adapt the Articles to the Editorial Policy of the Journal. Once the Article is accepted in its final version, the Journal will send the author the proofs for review. ECORFAN® will only accept the correction of errata and errors or omissions arising from the editing process of the Journal, reserving in full the copyrights and content dissemination. No deletions, substitutions or additions that alter the formation of the Article will be accepted.

Code of Ethics - Good Practices and Declaration of Solution to Editorial Conflicts

Declaration of Originality and unpublished character of the Article, of Authors, on the obtaining of data and interpretation of results, Acknowledgments, Conflict of interests, Assignment of rights and Distribution

The ECORFAN-Mexico, S.C Management claims to Authors of Articles that its content must be original, unpublished and of Scientific, Technological and Innovation content to be submitted for evaluation.

The Authors signing the Article must be the same that have contributed to its conception, realization and development, as well as obtaining the data, interpreting the results, drafting and reviewing it. The Corresponding Author of the proposed Article will request the form that follows.

Article title:

– The sending of an Article to Journal of Quantitative and Statistical Analysis emanates the commitment of the author not to submit it simultaneously to the consideration of other series publications for it must complement the Format of Originality for its Article, unless it is rejected by the Arbitration Committee, it may be withdrawn.

– None of the data presented in this article has been plagiarized or invented. The original data are clearly distinguished from those already published. And it is known of the test in PLAGSCAN if a level of plagiarism is detected Positive will not proceed to arbitrate.

– References are cited on which the information contained in the Article is based, as well as theories and data from other previously published Articles.

– The authors sign the Format of Authorization for their Article to be disseminated by means that ECORFAN-Mexico, S.C. In its Holding Bolivia considers pertinent for disclosure and diffusion of its Article its Rights of Work.

– Consent has been obtained from those who have contributed unpublished data obtained through verbal or written communication, and such communication and Authorship are adequately identified.

– The Author and Co-Authors who sign this work have participated in its planning, design and execution, as well as in the interpretation of the results. They also critically reviewed the paper, approved its final version and agreed with its publication.

– No signature responsible for the work has been omitted and the criteria of Scientific Authorization are satisfied.

– The results of this Article have been interpreted objectively. Any results contrary to the point of view of those who sign are exposed and discussed in the Article.

Copyright and Access

The publication of this Article supposes the transfer of the copyright to ECORFAN-Mexico, SC in its Holding Bolivia for it Journal of Quantitative and Statistical Analysis, which reserves the right to distribute on the Web the published version of the Article and the making available of the Article in This format supposes for its Authors the fulfilment of what is established in the Law of Science and Technology of the United Mexican States, regarding the obligation to allow access to the results of Scientific Research.

Article Title:

Name and Surnames of the Contact Author and the Coauthors	Signature
1.	
2.	
3.	
4.	

Principles of Ethics and Declaration of Solution to Editorial Conflicts

Editor Responsibilities

The Publisher undertakes to guarantee the confidentiality of the evaluation process, it may not disclose to the Arbitrators the identity of the Authors, nor may it reveal the identity of the Arbitrators at any time.

The Editor assumes the responsibility to properly inform the Author of the stage of the editorial process in which the text is sent, as well as the resolutions of Double-Blind Review.

The Editor should evaluate manuscripts and their intellectual content without distinction of race, gender, sexual orientation, religious beliefs, ethnicity, nationality, or the political philosophy of the Authors.

The Editor and his editing team of ECORFAN® Holdings will not disclose any information about Articles submitted to anyone other than the corresponding Author.

The Editor should make fair and impartial decisions and ensure a fair Double-Blind Review.

Responsibilities of the Editorial Board

The description of the peer review processes is made known by the Editorial Board in order that the Authors know what the evaluation criteria are and will always be willing to justify any controversy in the evaluation process. In case of Plagiarism Detection to the Article the Committee notifies the Authors for Violation to the Right of Scientific, Technological and Innovation Authorization.

Responsibilities of the Arbitration Committee

The Arbitrators undertake to notify about any unethical conduct by the Authors and to indicate all the information that may be reason to reject the publication of the Articles. In addition, they must undertake to keep confidential information related to the Articles they evaluate.

Any manuscript received for your arbitration must be treated as confidential, should not be displayed or discussed with other experts, except with the permission of the Editor.

The Arbitrators must be conducted objectively, any personal criticism of the Author is inappropriate.

The Arbitrators must express their points of view with clarity and with valid arguments that contribute to the Scientific, Technological and Innovation of the Author.

The Arbitrators should not evaluate manuscripts in which they have conflicts of interest and have been notified to the Editor before submitting the Article for Double-Blind Review.

Responsibilities of the Authors

Authors must guarantee that their articles are the product of their original work and that the data has been obtained ethically.

Authors must ensure that they have not been previously published or that they are not considered in another serial publication.

Authors must strictly follow the rules for the publication of Defined Articles by the Editorial Board.

The authors have requested that the text in all its forms be an unethical editorial behavior and is unacceptable, consequently, any manuscript that incurs in plagiarism is eliminated and not considered for publication.

Authors should cite publications that have been influential in the nature of the Article submitted to arbitration.

Information services

Indexation - Bases and Repositories

LATINDEX (Scientific Journals of Latin America, Spain and Portugal)
RESEARCH GATE (Germany)
GOOGLE SCHOLAR (Citation indices-Google)
REDIB (Ibero-American Network of Innovation and Scientific Knowledge- CSIC)
MENDELEY (Bibliographic References Manager)

Publishing Services:

Citation and Index Identification H.
Management of Originality Format and Authorization.
Testing Article with PLAGSCAN.
Article Evaluation.
Certificate of Double-Blind Review.
Article Edition.
Web layout.
Indexing and Repository
ArticleTranslation.
Article Publication.
Certificate of Article.
Service Billing.

Editorial Policy and Management

21 Santa Lucía, CP-5220. Libertadores -Sucre–Bolivia. Phones: +52 1 55 6159 2296, +52 1 55 1260 0355, +52 1 55 6034 9181; Email: contact@ecorfan.org www.ecorfan.org

Journal of Quantitative and Statistical Analysis

2410 3438
ISSN 2410 - 3438